

Influence of the catalyst structure in the cycloaddition of oxiranes and isocyanates promoted by tetraarylstibonium cations

Mengxi Yang, Nilanjana Pati, Guillaume Bélanger-Chabot, and François P. Gabbaï*

^aDepartment of Chemistry, Texas A&M University, College Station, Texas 77843-3255, United States.

Email: francois@tamu.edu

This PDF file includes:

| | |
|--|-----|
| Figure S1. ¹ H NMR of 2 [OTf] in CDCl ₃ | S3 |
| Figure S2. ¹³ C NMR of 2 [OTf] in CDCl ₃ | S4 |
| Figure S3. ¹⁹ F NMR of 2 [OTf] in CDCl ₃ | S4 |
| Figure S4. Crystal structure of 2 ⁺ in 2 [OTf]..... | S4 |
| Figure S5. ¹ H NMR of 4 [OTf] in CDCl ₃ | S5 |
| Figure S6. ¹³ C NMR of 4 [OTf] in CDCl ₃ | S5 |
| Figure S7. ¹⁹ F NMR of 4 [OTf] in CDCl ₃ | S5 |
| Figure S8. ¹ H NMR of 5 [OTf] in CDCl ₃ | S6 |
| Figure S9. ¹³ C NMR of 5 [OTf] in CDCl ₃ | S6 |
| Figure S10. ¹⁹ F NMR of 5 [OTf] in CDCl ₃ | S6 |
| Figure S11. ¹ H NMR of 6 [OTf] in CDCl ₃ | S7 |
| Figure S12. ¹³ C NMR of 6 [OTf] in CDCl ₃ | S7 |
| Figure S13. ¹⁹ F NMR of 6 [OTf] in CDCl ₃ | S7 |
| Figure S14. ¹⁹ F NMR of 7 [SbCl ₆] in CD ₃ CN..... | S8 |
| Figure S15. ¹³ C NMR of 7 [SbCl ₆] in CD ₃ CN..... | S8 |
| Figure S16. Representative ¹ H NMR spectrum collected during the experiment presented in Table 1, Entry 1..... | S9 |
| Figure S17. Representative ¹ H NMR spectrum collected during the experiment presented in Table 1, Entry 2..... | S10 |
| Figure S18. Representative ¹ H NMR spectrum collected during the experiment presented in Table 1, Entry 3..... | S10 |
| Figure S19. Representative ¹ H NMR spectrum collected during the experiment presented in Table 1, Entry 4..... | S11 |
| Figure S20. Representative ¹ H NMR spectrum collected during the experiment presented in Table 1, Entry 5..... | S11 |
| Figure S21. Representative ¹ H NMR spectrum collected during the experiment presented in Table 1, Entry 6..... | S12 |
| Figure S22. Representative ¹ H NMR spectrum collected during the experiment presented in Table 1, Entry 7..... | S12 |
| Figure S23. Representative ¹ H NMR spectrum collected during the experiment presented in Table 1, Entry 8..... | S13 |
| Figure S23. ¹ H NMR of the stoichiometric reaction of 5 [OTf] and propylene oxide..... | S13 |
| Figure S23. ¹ H NMR of the stoichiometric reaction of 6 [OTf] and propylene oxide..... | S14 |
| Figure S24. Representative ¹ H NMR spectrum collected during the experiment presented in Table 2, Entry 1..... | S15 |
| Figure S25. Representative ¹ H NMR spectrum collected during the experiment presented in Table 2, Entry 2..... | S15 |
| Figure S26. Representative ¹ H NMR spectrum collected during the experiment presented in Table 2, Entry 3..... | S16 |
| Figure S27. Representative ¹ H NMR spectrum collected during the experiment presented in Table 2, Entry 4..... | S17 |
| Figure S28. Representative ¹ H NMR spectrum collected during the experiment presented in Table 2, Entry 5..... | S18 |
| Figure S29. Representative ¹ H NMR spectrum collected during the experiment presented in Table 2, Entry 6..... | S18 |
| Figure S30. ¹ H NMR of 4-methyl-3-phenyl-2-oxazolidinone (A1) in CDCl ₃ | S19 |
| Figure S31. ¹³ C NMR of 4-methyl-3-phenyl-2-oxazolidinone (A1) in CDCl ₃ | S20 |
| Figure S32. ¹ H NMR of 5-methyl-3-phenyl-2-oxazolidinone (B1) in CDCl ₃ | S20 |
| Figure S33. ¹³ C NMR of 5-methyl-3-phenyl-2-oxazolidinone (B1) in CDCl ₃ | S21 |
| Figure S34. ¹ H NMR of 3,4-diphenyl-2-oxazolidinone (A2) in CDCl ₃ | S22 |

| | |
|---|-----|
| Figure S35. ^{13}C NMR of 3,4-diphenyl-2-oxazolidinone (A2) in CDCl_3 | S23 |
| Figure S36. ^1H NMR of 3,5-diphenyl-2-oxazolidinone (B2) in CDCl_3 | S23 |
| Figure S37. ^{13}C NMR of 3,5-diphenyl-2-oxazolidinone (B2) in CDCl_3 | S24 |
| Table S1. Crystal data, data collection, and structure refinement for 2 [OTf] | S25 |
| Table S2. Crystal data, data collection, and structure refinement for 4 [OTf] | S26 |
| Table S3. Crystal data, data collection, and structure refinement for 5 [OTf] | S27 |
| Table S4. Crystal data, data collection, and structure refinement for 6 [OTf] | S28 |
| Table S5. Crystal data, data collection, and structure refinement for 7 [SbCl_6] | S29 |
| Table S6. XYZ coordinates of the optimized geometry of 5 $^+$ | S30 |
| Table S7. XYZ coordinates of the optimized geometry of 6 $^+$ | S31 |

1 Experimental Section

1.1 Synthesis of 1-Naphthyltriphenylstibonium triflate (2[OTf])

2[OTf] has been previously described.¹ As part of the current study, it was prepared as follows. A 100 mL Schlenk flask was charged with 1-bromonaphthalene (600 mg, 2.4 mmol, 1 eq) and 15 mL THF. The solution was cooled to -78 °C and treated with ⁿBuLi (2.65 M in hexanes, 1.0 mL, 2.6 mmol, 1.1 eq) which was added drop-wise. The resulting bright yellow solution was stirred at -78 °C for 1 h. Next, the solution was transferred drop wise to a Ph₃SbBr₂ (1.20g, 2.4 mmol, 1 eq) solution in mixed solvents (6 mL THF, 30 mL Et₂O) at -78 °C. The reaction mixture, which turned dark yellow, was allowed to warm to room temperature overnight, resulting in a pale-yellow solution. The solvent was removed *in vacuo* to afford an oily solid, which was dissolved in CH₂Cl₂ and passed through a short plug of Celite in air. After removing CH₂Cl₂ *in vacuo*, the solid was extracted with methanol and passed through a second plug of Celite in air. Removal of the solvent *in vacuo* afforded a pale-yellow solid which was used without further purification. This solid was dissolved in CH₂Cl₂ (15 mL) and treated with solid AgOTf (380 mg, 1.5 mmol, 0.6 eq) under N₂ atmosphere. The resulting yellow suspension was allowed to stir at room temperature in the dark for 2 h. The suspension was then filtered over Celite, and the filtrate was reduced and purified by flash chromatography over silica gel (100% ethyl acetate). The second major fraction was collected and washed with hexanes to yield 2[OTf] as air- and moisture- stable white powder (551 mg, 37% yield based on Ph₃SbBr₂).

2[OTf]: ¹H NMR (500 MHz, CDCl₃) δ = 8.33 – 8.24 (m, 1H), 8.14 – 8.05 (m, 1H), 7.86 – 7.55 (m, 19H), 7.55 – 7.45 (m, 1H). ¹³C NMR (126 MHz, CDCl₃) δ = 137.75 (s, naphthyl), 135.72 (s, *o*-Ph), 134.77 (s, naphthyl), 133.92 (s, *p*-Ph), 131.47 (s, *m*-Ph), 130.28 (s, naphthyl), 129.00 (s, naphthyl), 127.80 (s, naphthyl), 126.94 (s, naphthyl), 126.81 (s, naphthyl), 123.17 (s, quaternary, Ph), 120.72 (q, *J*_{C-F} = 324.8, OTf). ¹⁹F NMR (470 MHz, CDCl₃) δ = -78.74 (s, OTf). Spectral data are in accord with the previous report.¹ Single crystals suitable for X-ray diffraction were obtained by slow evaporation of hexanes into a CDCl₃ solution in air.

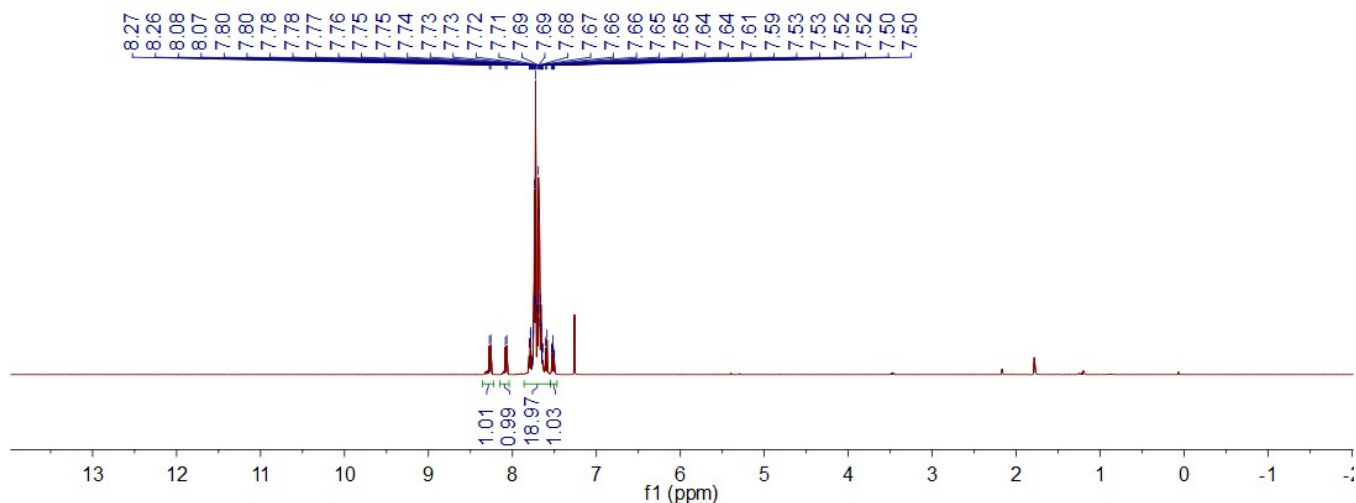


Figure S1. ¹H NMR of 2[OTf] in CDCl₃.

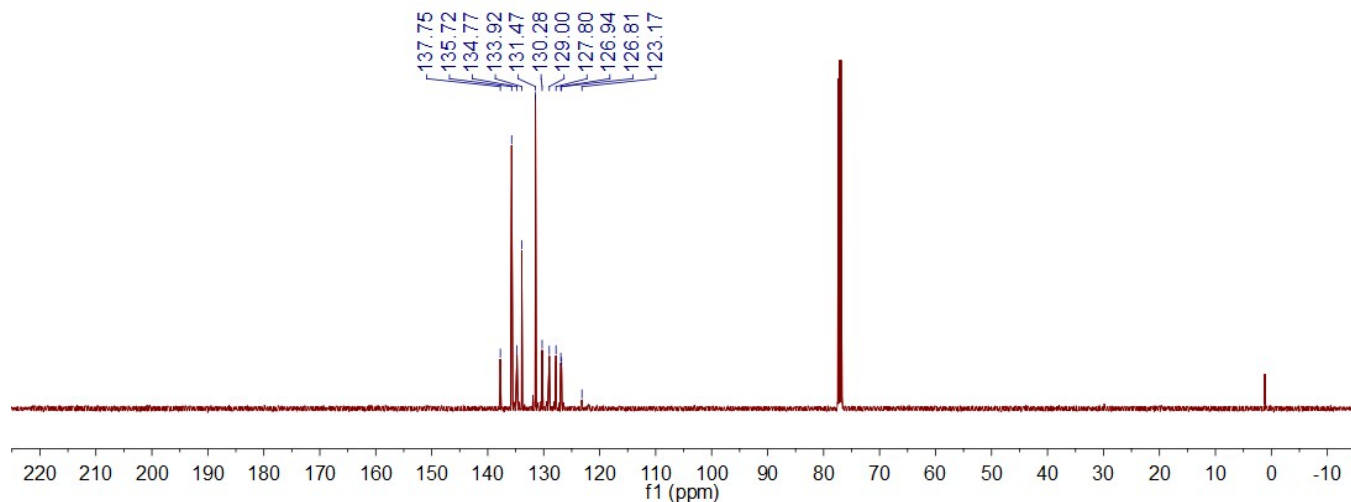


Figure S2. ^{13}C NMR of $2[\text{OTf}]$ in CDCl_3 .

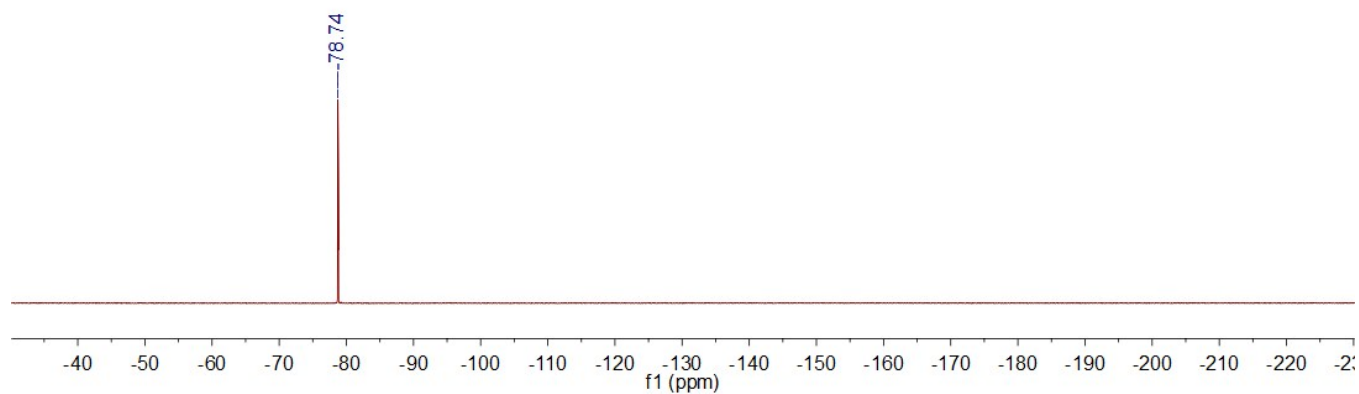


Figure S3. ^{19}F NMR of $2[\text{OTf}]$ in CDCl_3 .

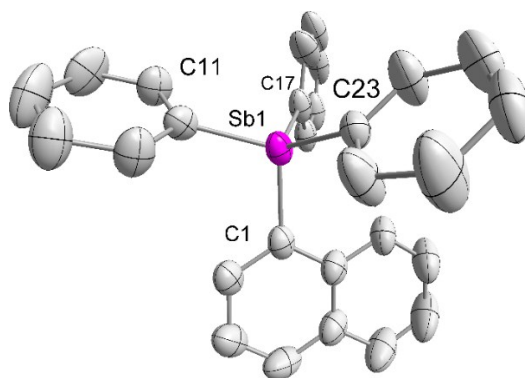


Figure S4. Crystal structure of 2^+ in $2[\text{OTf}]$.

Ellipsoids are drawn at a 50% probability level. The triflate counteranion and the hydrogen atoms are omitted for clarity. Selected bond lengths (\AA) and angles ($^\circ$): $\text{Sb1-C1} = 2.086(4)$, $\text{Sb1-C11} = 2.085(4)$, $\text{Sb1-C17} = 2.098(4)$, $\text{Sb1-C23} = 2.091(4)$, $\angle\text{C1-Sb1-C11} = 107.0(2)$, $\angle\text{C1-Sb1-C17} = 112.1(2)$, $\angle\text{C1-Sb1-C23} = 104.2(2)$, $\angle\text{C11-Sb1-C17} = 108.1(2)$, $\angle\text{C11-Sb1-C23} = 114.1(2)$, $\angle\text{C17-Sb1-C23} = 111.3(2)$.

1.2 NMR spectra of 4-6[OTf], 7[SbCl₆]

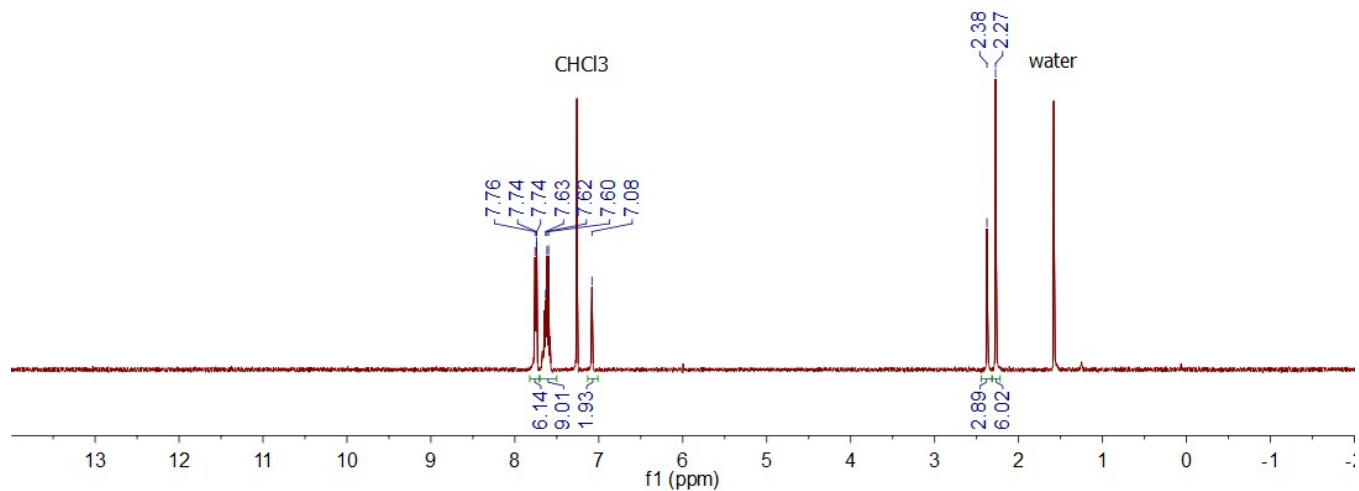


Figure S5. ¹H NMR of 4[OTf] in CDCl₃.

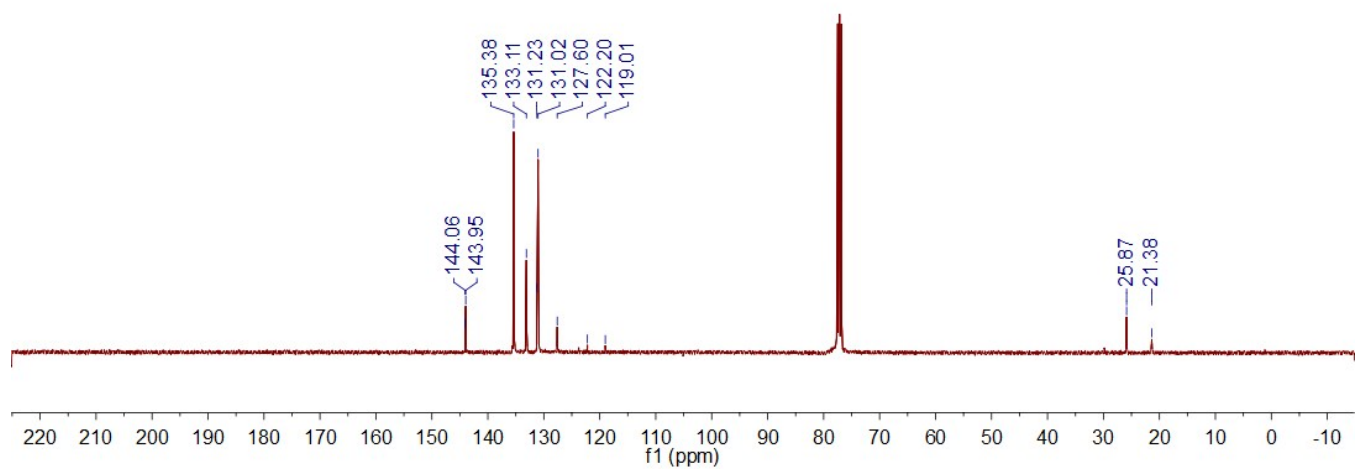


Figure S6. ¹³C NMR of 4[OTf] in CDCl₃.

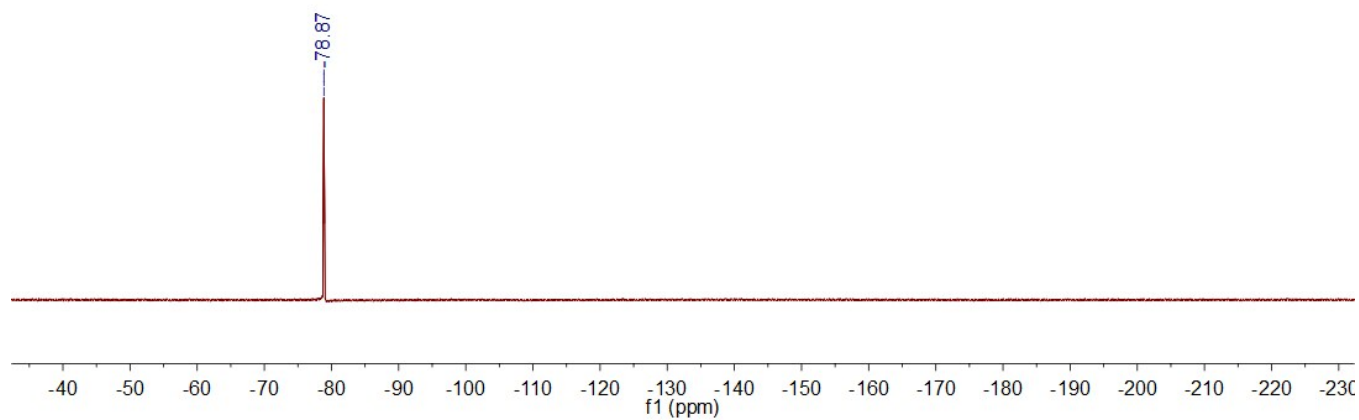


Figure S7. ¹⁹F NMR of 4[OTf] in CDCl₃.

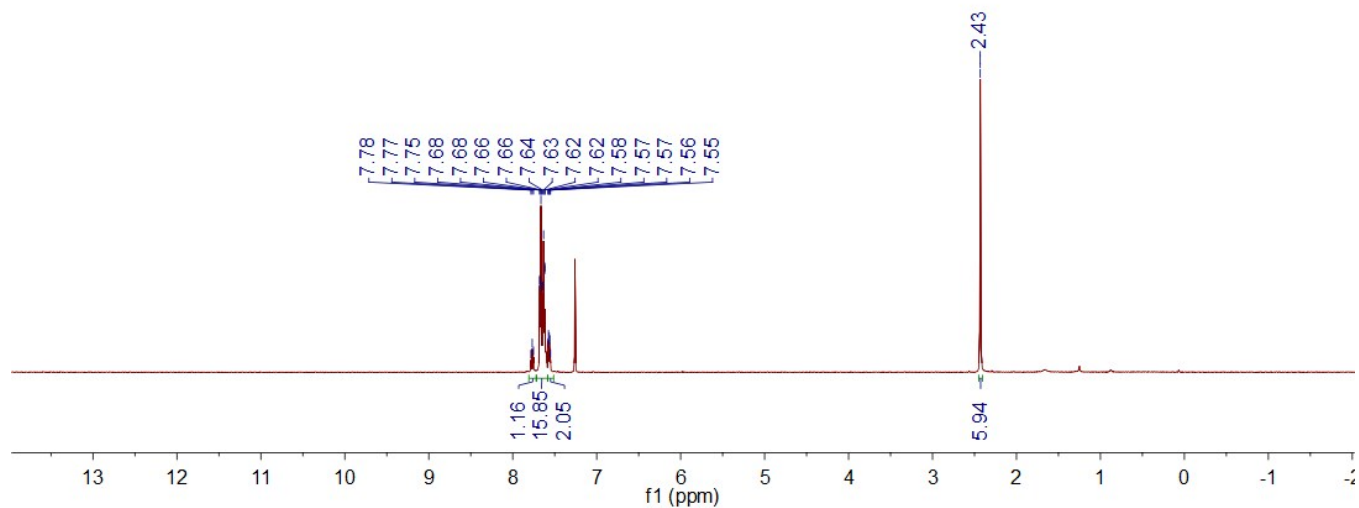


Figure S8. ^1H NMR of 5[OTf] in CDCl_3 .

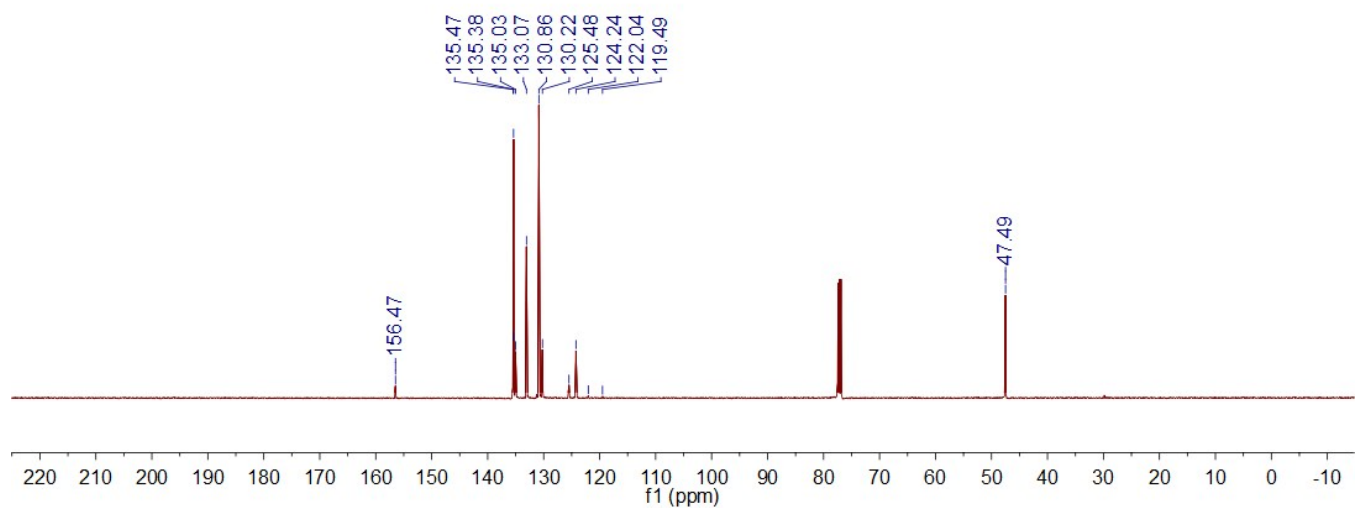


Figure S9. ^{13}C NMR of 5[OTf] in CDCl_3 .

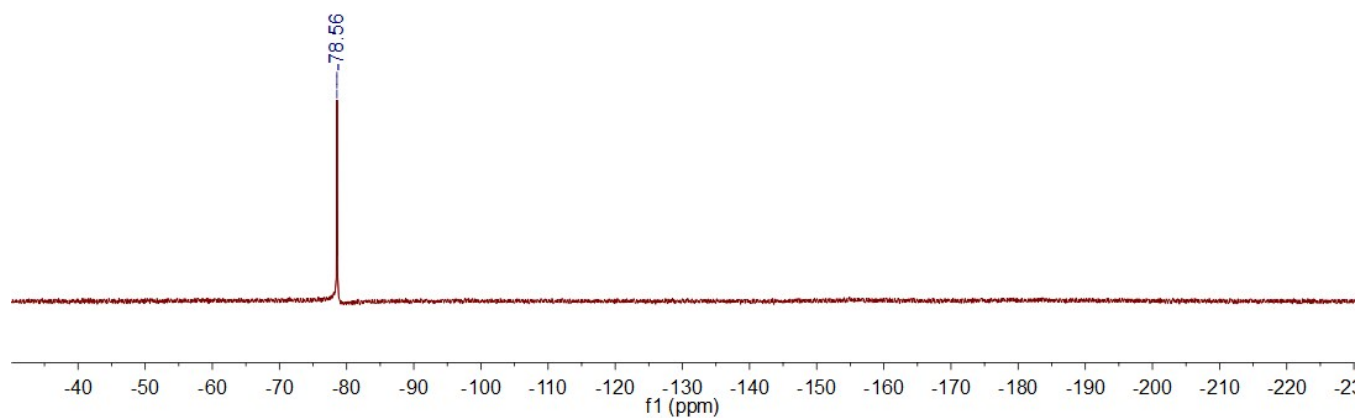


Figure S10. ^{19}F NMR of 5[OTf] in CDCl_3 .

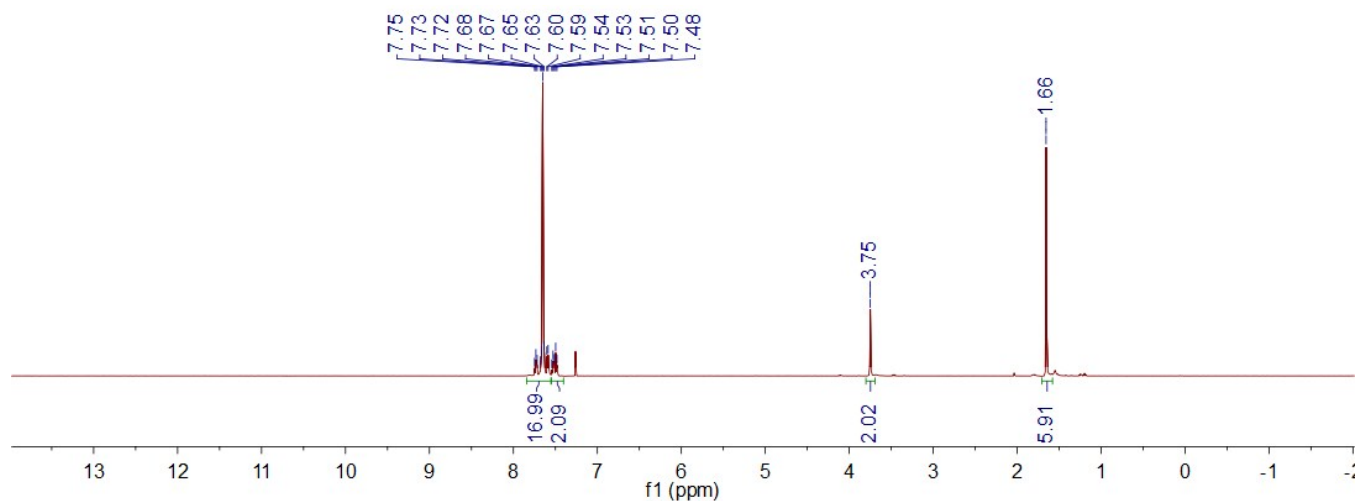


Figure S11. ^1H NMR of $6[\text{OTf}]$ in CDCl_3 .

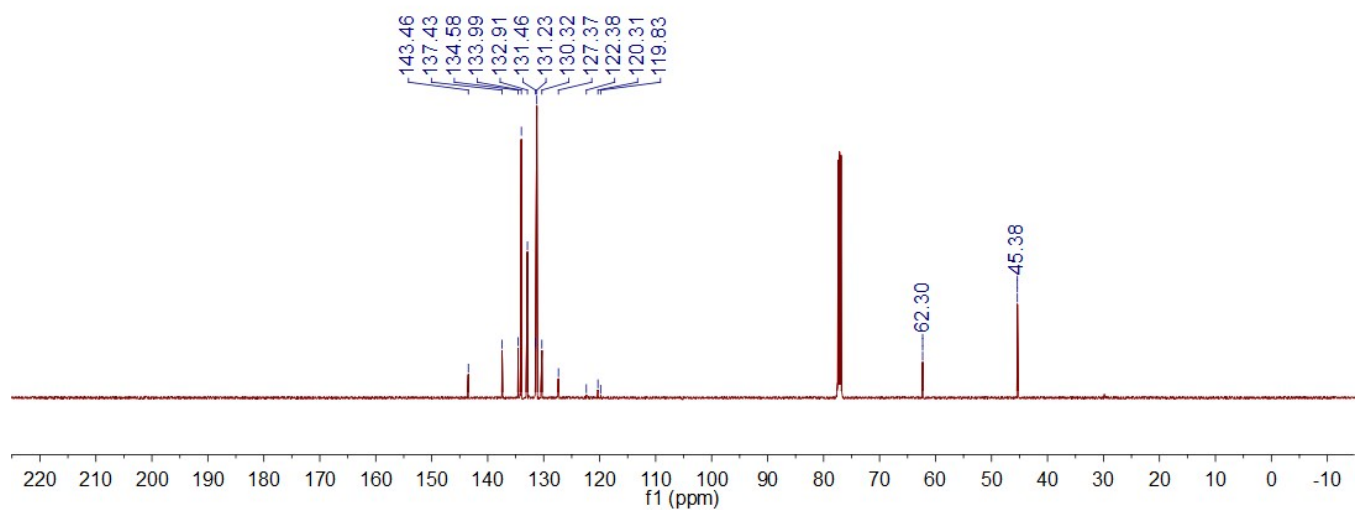


Figure S12. ^{13}C NMR of $6[\text{OTf}]$ in CDCl_3 .

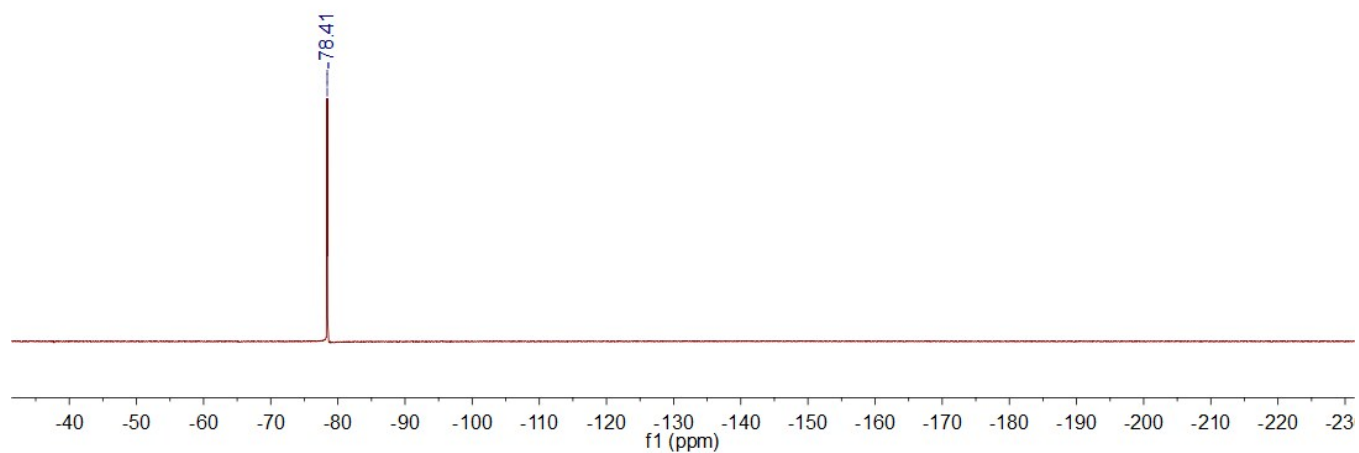


Figure S13. ^{19}F NMR of $6[\text{OTf}]$ in CDCl_3 .

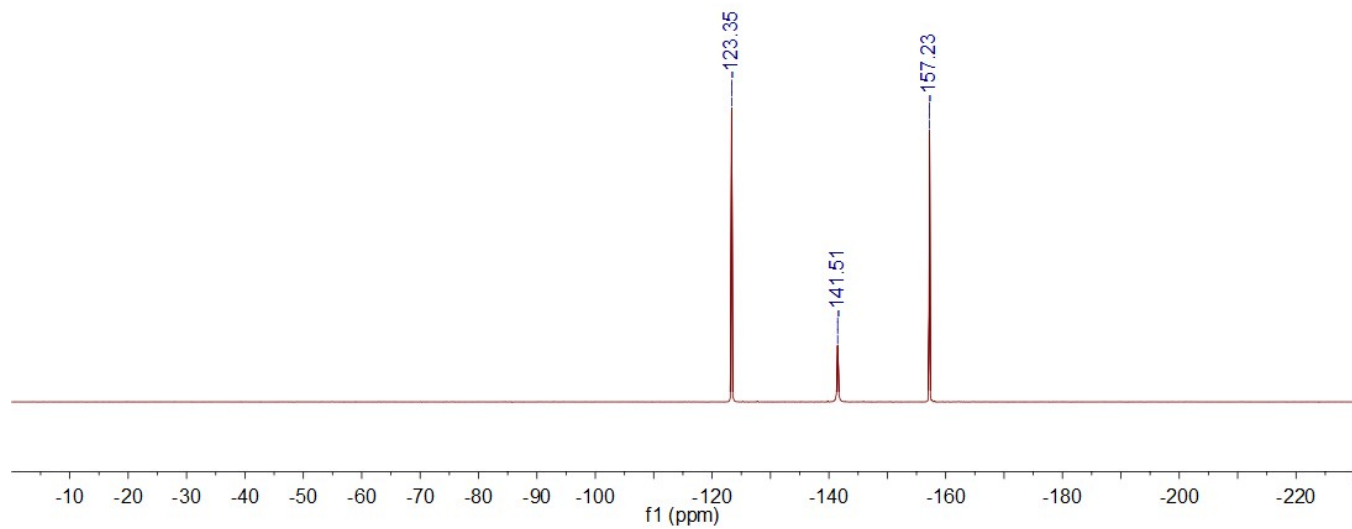


Figure S14. ^{19}F NMR of $7[\text{SbCl}_6]$ in CD_3CN .

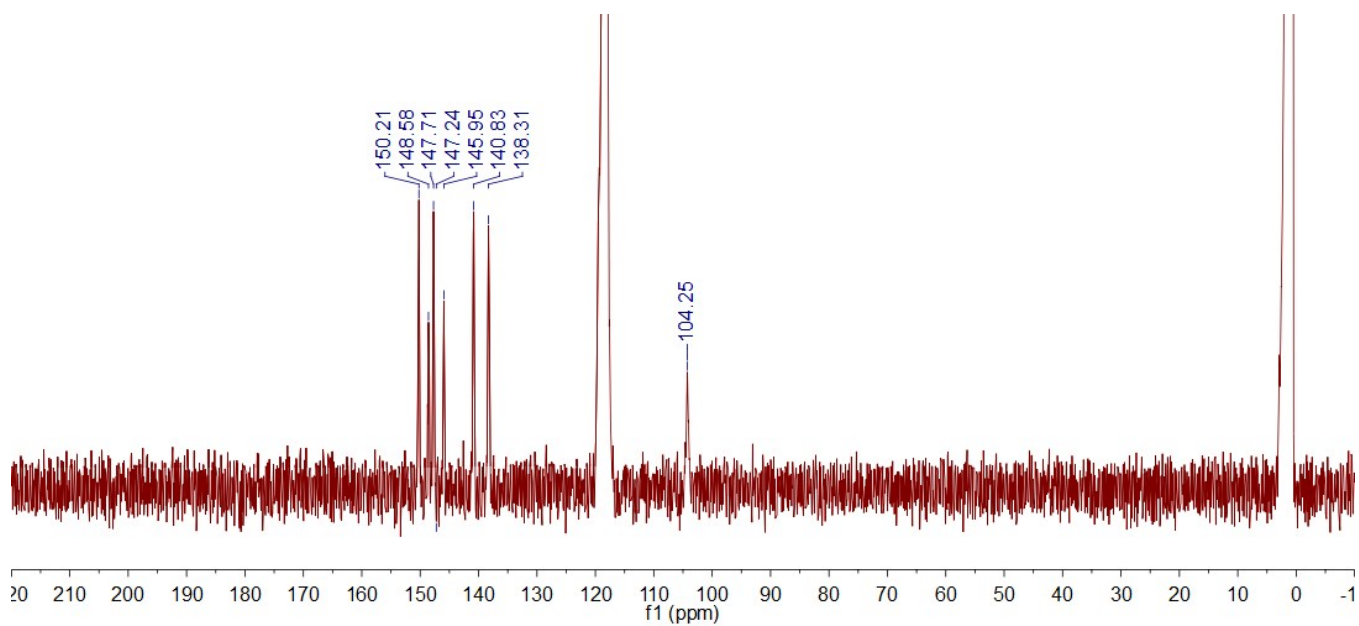
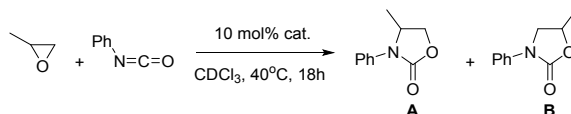


Figure S15. ^{13}C NMR of $7[\text{SbCl}_6]$ in CD_3CN .

1.3 Catalytic cycloaddition of oxiranes and isocyanates in NMR scale.

For each entry in Table s 1-2, the yield and selectivity are reported as the average result across multiple data points, only one representative ^1H NMR spectrum for each entry is shown below.

1.3.1 *In situ* NMR spectra collected during the experiments presented in Table 1.



The formation of the products was monitored by ^1H NMR *in situ*. The integration of the resonance at 3.0 ppm (m, 12H) of the tetrabutylammonium cation was used as a standard. The yield of the major isomer A was calculated based on the integration of two resonances: 4.4 ppm (m, 2H) and 3.8 ppm (m, 1H). The yield of the minor isomer B was calculated based on the integration of three resonances: 4.6 ppm (m, 1H), 4.0 ppm (t, 1H), and 3.5 ppm (dd, 1H). An impurity in the reaction mixture gives three resonances in the 2.5 – 5.0 ppm region, two of which overlap with isomer A: 4.7 ppm (1H), 4.4 ppm (1H) and 3.8 ppm (1H).

Additionally, no reaction took place when catalysts **5**[OTf] and **6**[OTf] were mixed with a stoichiometric amount of propylene oxide in CDCl_3 over the course of 12 hours at 40°C . Spectra of these two stoichiometric experiments are provided below as well.

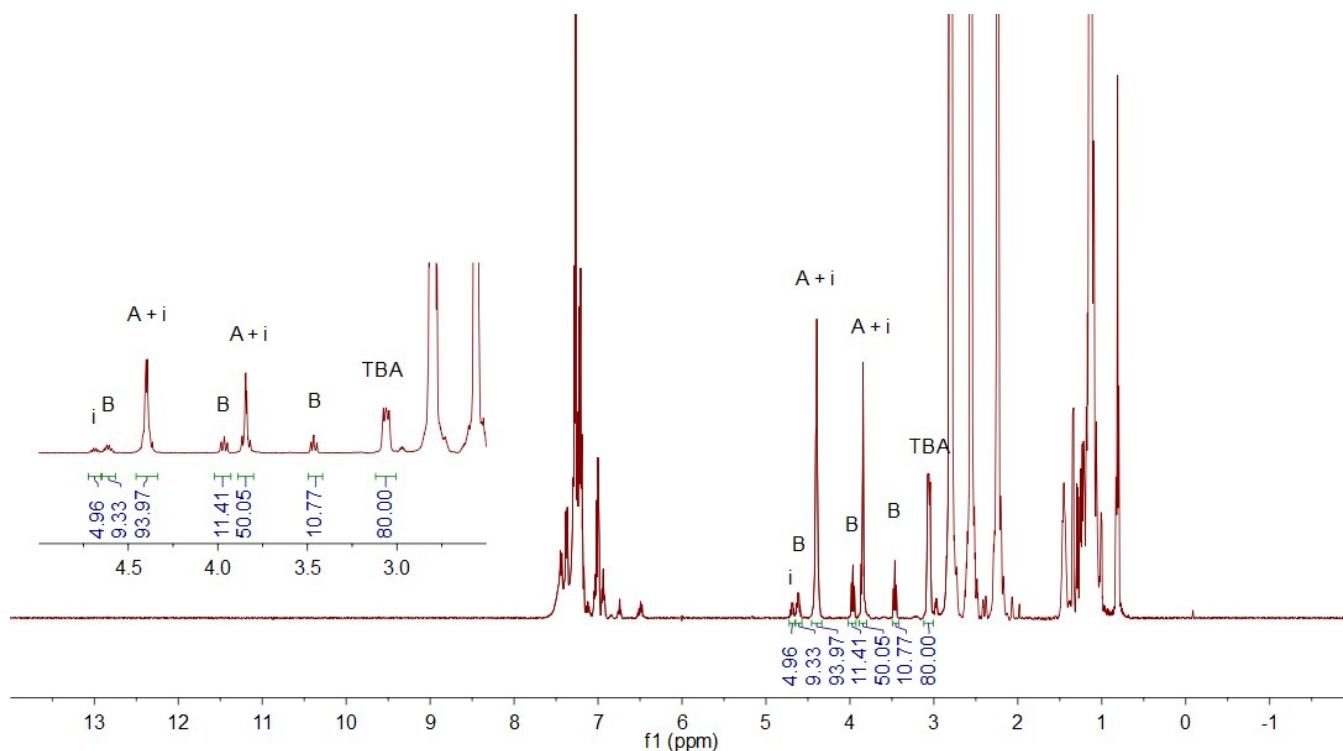


Figure S16. Representative ^1H NMR spectrum collected during the experiment presented in Table 1, Entry 1.

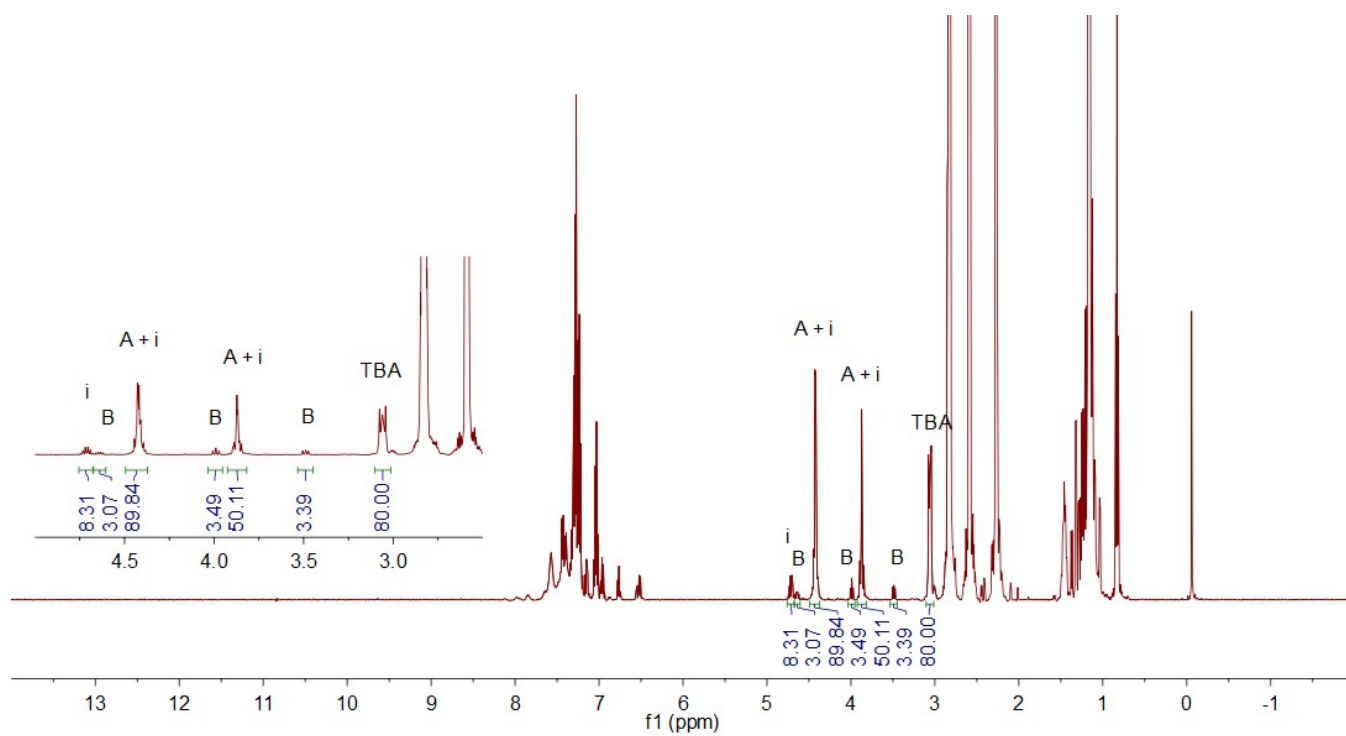


Figure S17. Representative ¹H NMR spectrum collected during the experiment presented in Table 1, Entry 2.

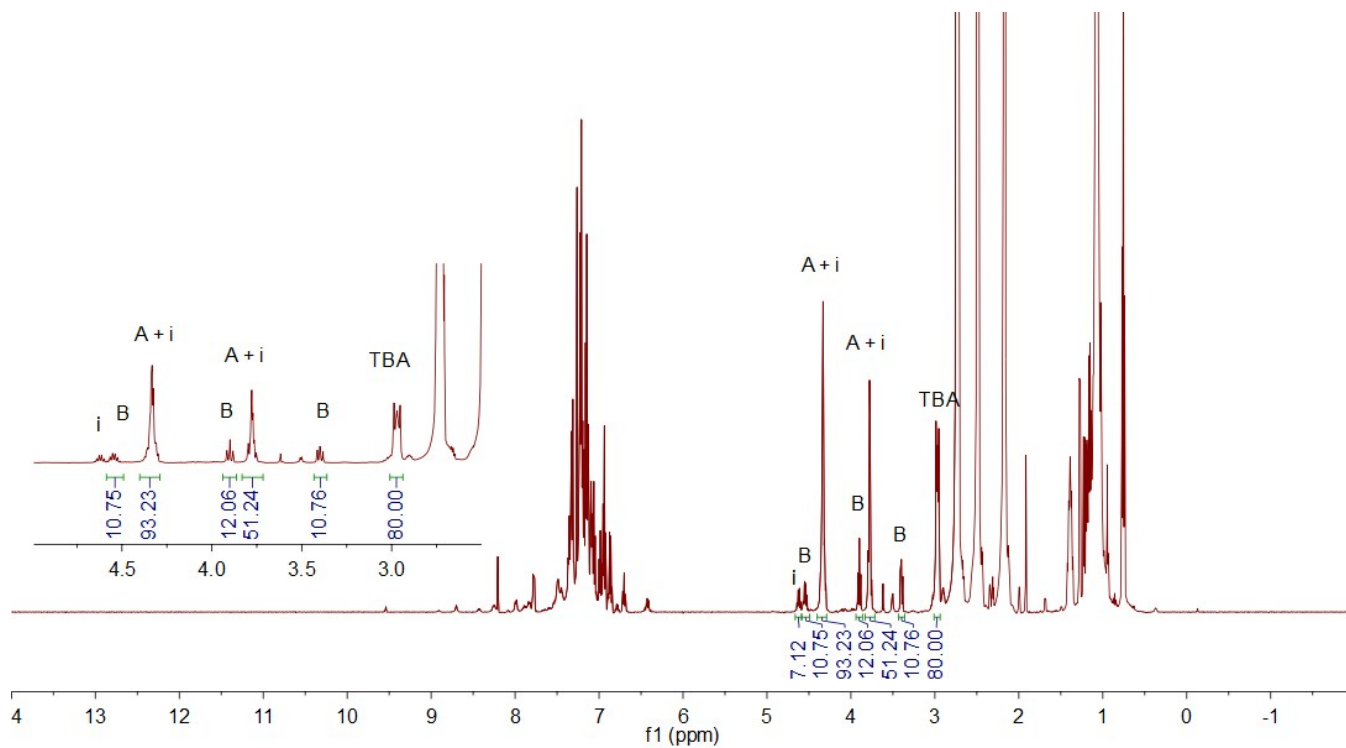


Figure S18. Representative ¹H NMR spectrum collected during the experiment presented in Table 1, Entry 3.

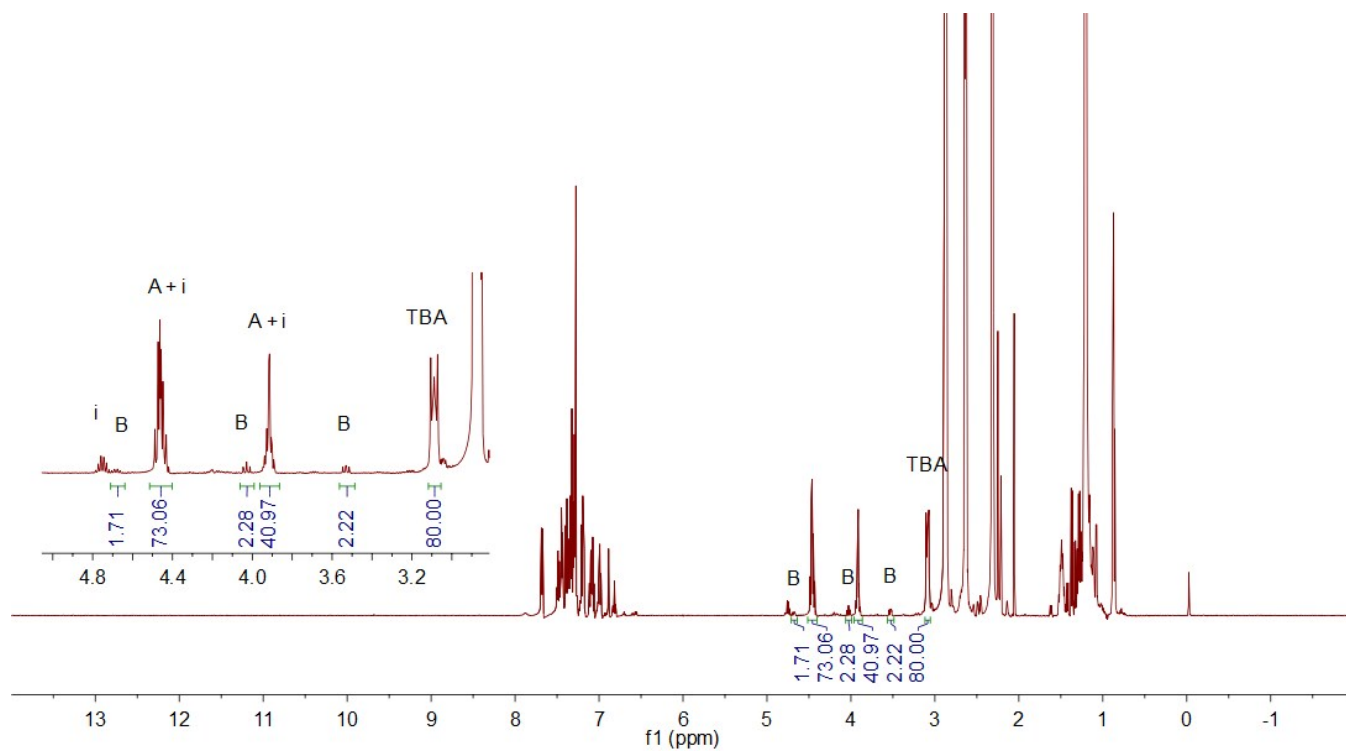


Figure S19. Representative ^1H NMR spectrum collected during the experiment presented in Table 1, Entry 4.

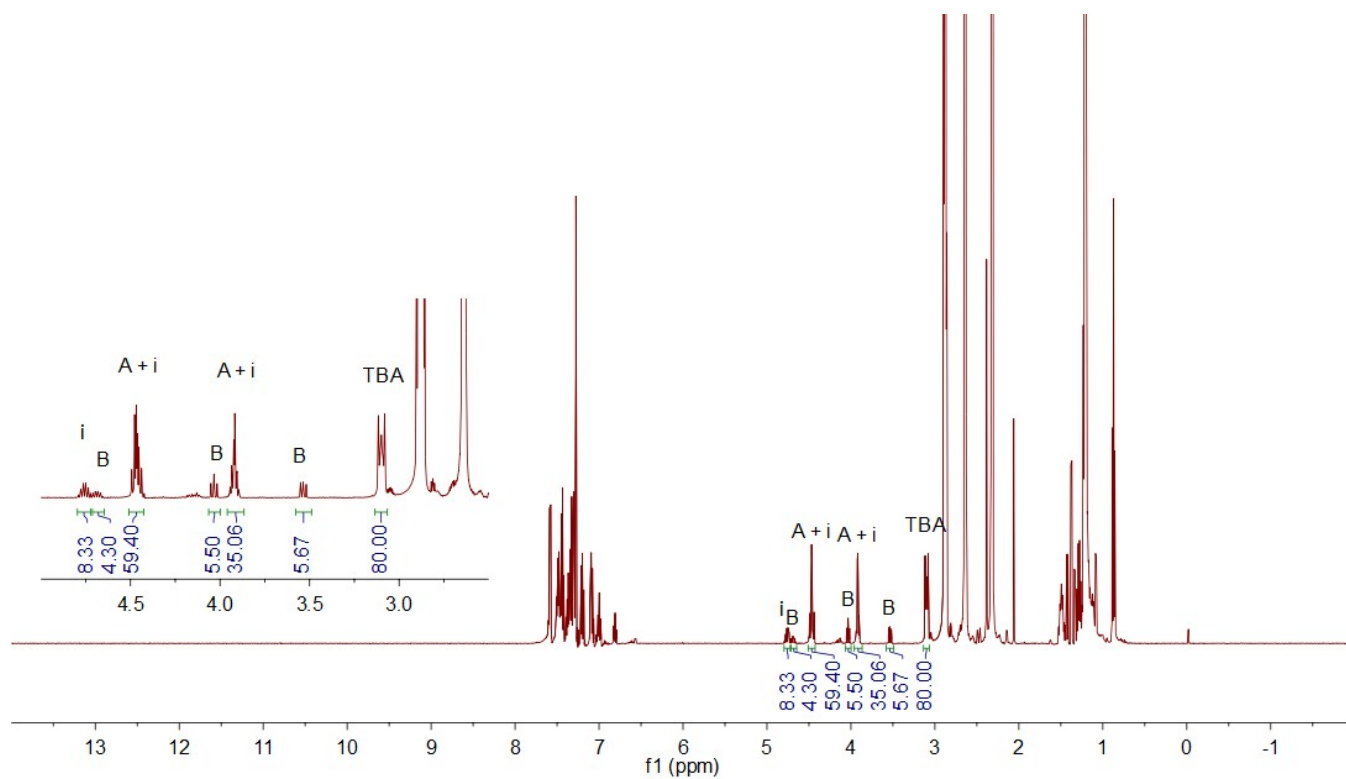


Figure S20. Representative ^1H NMR spectrum collected during the experiment presented in Table 1, Entry 5.

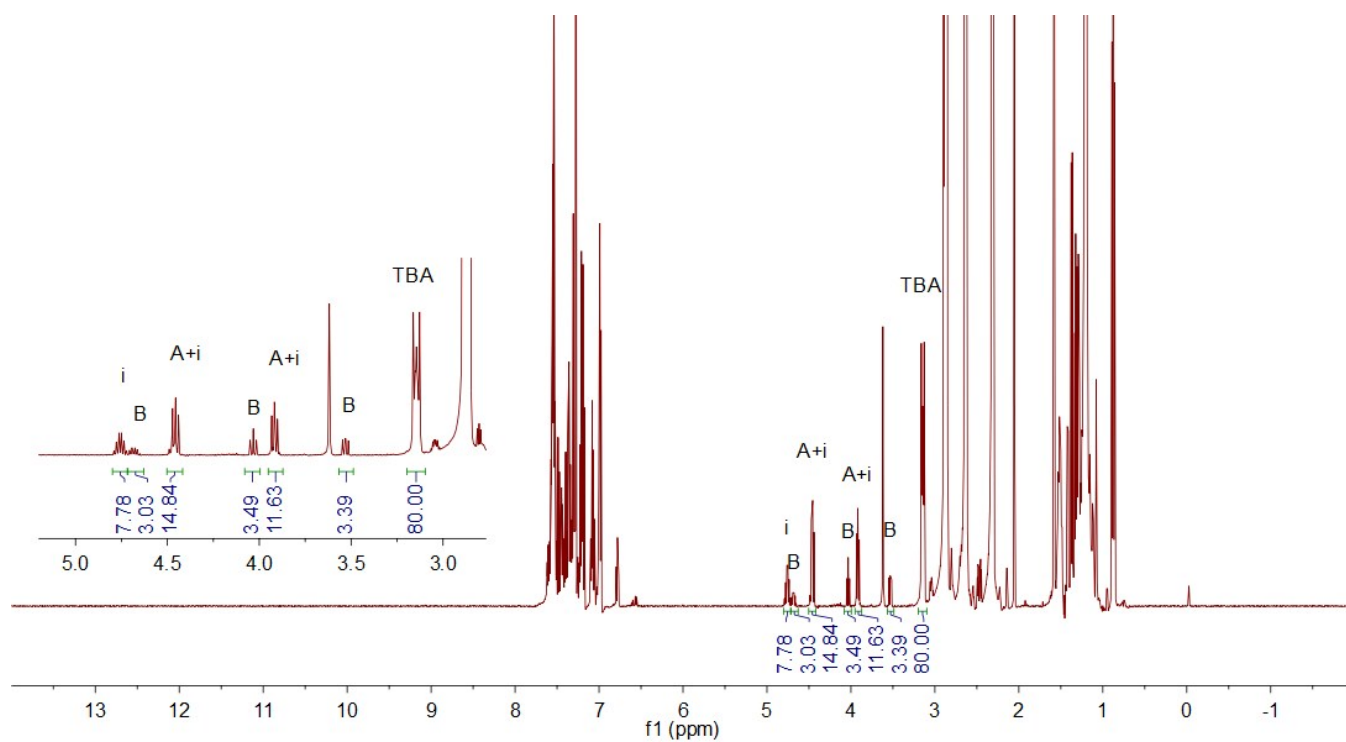


Figure S21. Representative ¹H NMR spectrum collected during the experiment presented in Table 1, Entry 6.

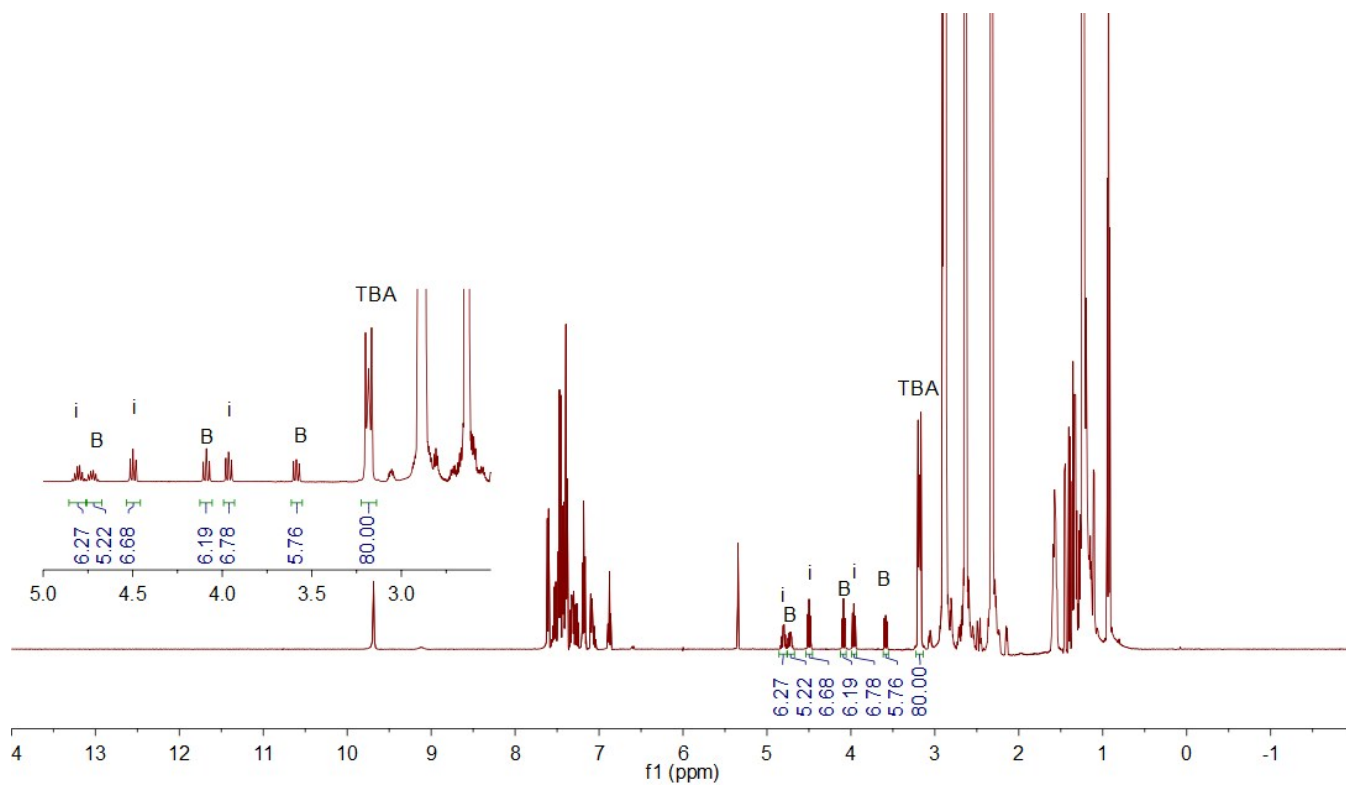


Figure S22. Representative ¹H NMR spectrum collected during the experiment presented in Table 1, Entry 7.

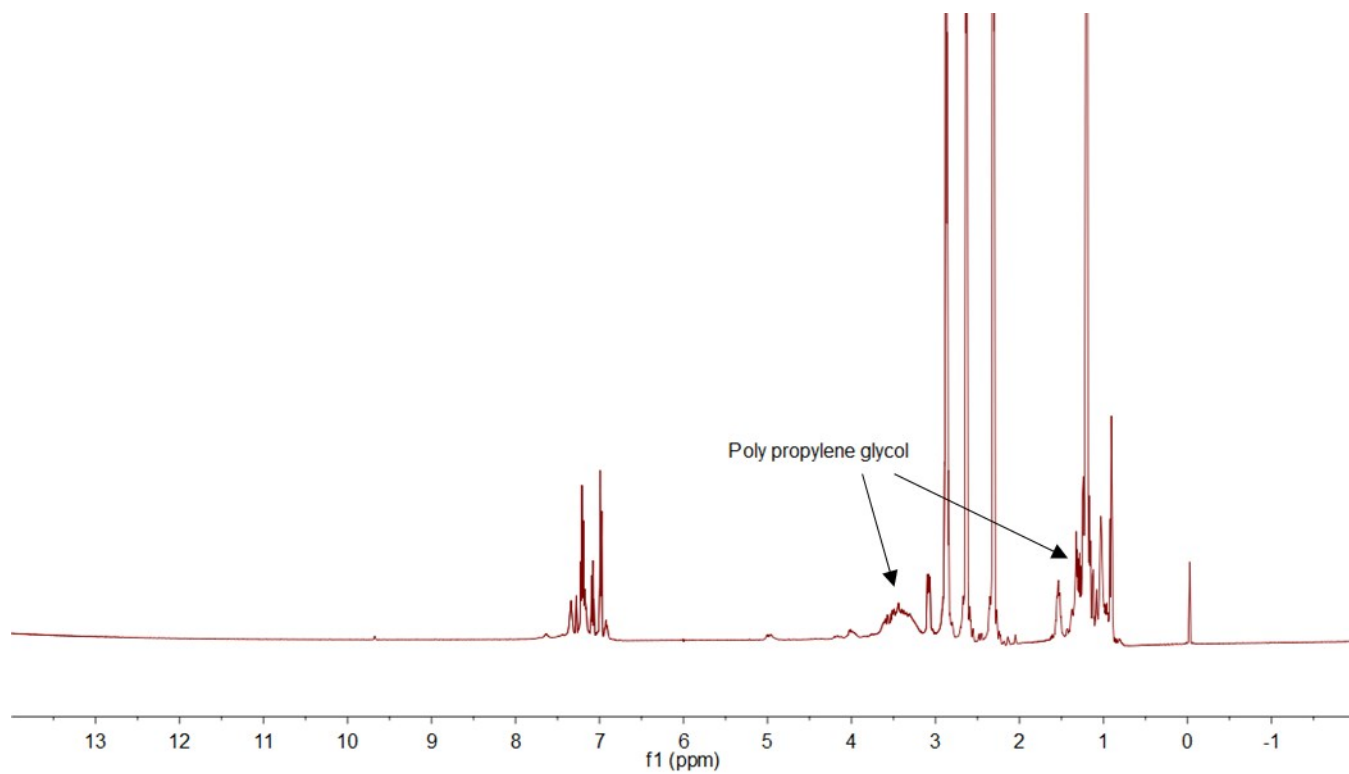


Figure S23. Representative ^1H NMR spectrum collected during the experiment presented in Table 1, Entry 8.

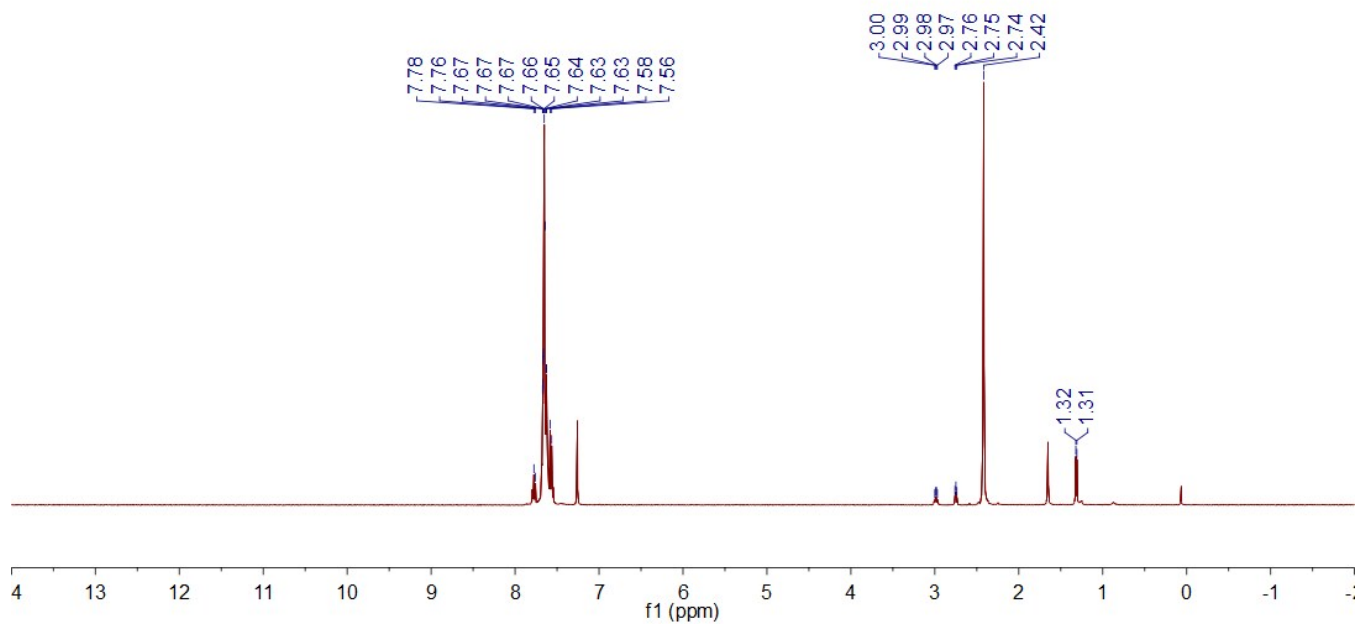


Figure S24. ^1H NMR of the stoichiometric reaction of 5[OTf] and propylene oxide.

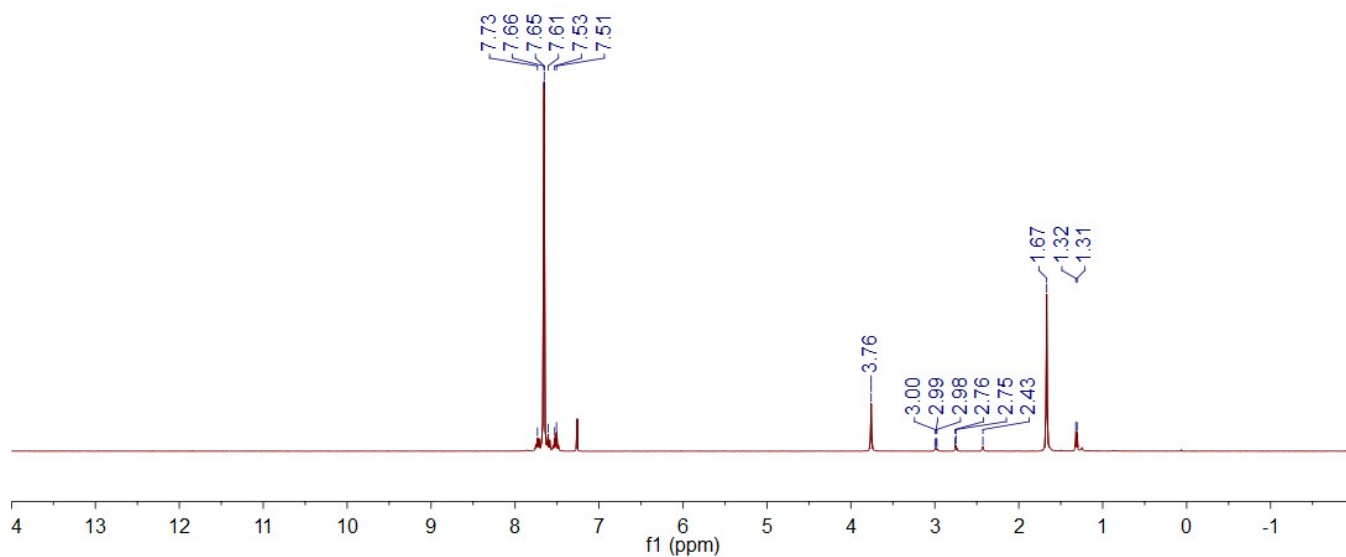
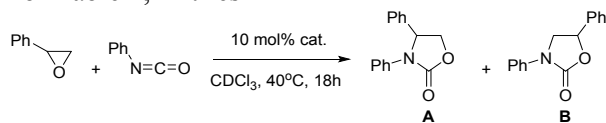


Figure S25. ^1H NMR of the stoichiometric reaction of **6**[OTf] and propylene oxide.

1.3.2 *In situ* NMR spectra collected during the experiments presented in Table 1.

1.3.2.1 *In situ* NMR spectrum of Table 2, Entries 1-2



The formation of the products was monitored by ^1H NMR *in situ*. The integration of the resonance at 1.5 ppm (m, 12H) of the tetrabutylammonium cation was used as a standard. The yield of the major isomer **A** was calculated based on the integration of three resonances: 5.4 ppm (dd, 1H), 4.7 ppm (t, 1H), and 4.2 ppm (dd, 1H). The yield of the minor isomer **B** was calculated based on the integration of three resonances: 5.6 ppm (dd, 1H), 4.7 ppm (t, 1H), and 4.3 ppm (dd, 1H).

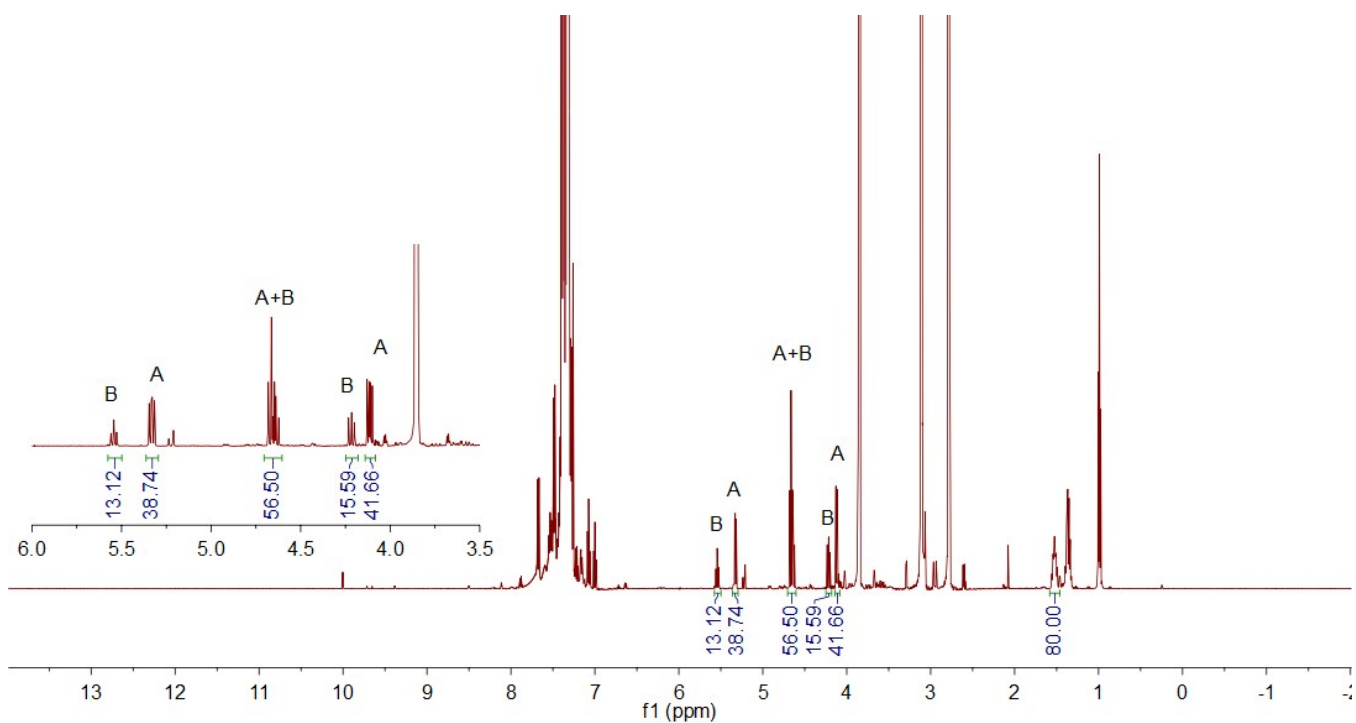


Figure S26. Representative ¹H NMR spectrum collected during the experiment presented in Table 2, Entry 1.

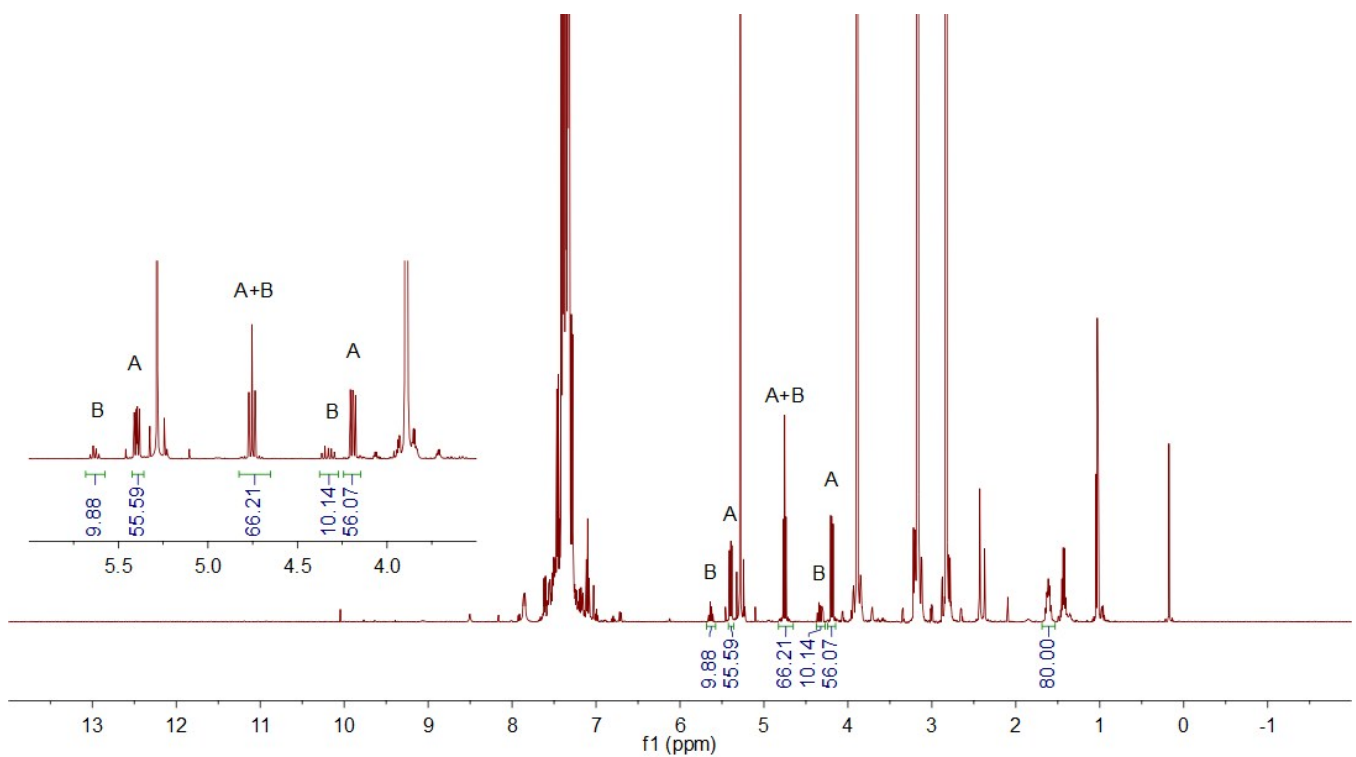
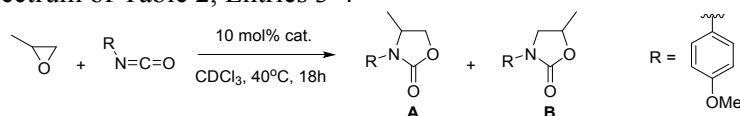


Figure S27. Representative ¹H NMR spectrum collected during the experiment presented in Table 2, Entry 2.

1.3.2.2 *In situ* NMR spectrum of Table 2, Entries 3-4



The formation of the products was monitored by ^1H NMR *in situ*. The integration of the resonance at 3.0 ppm (m, 12H) of the tetrabutylammonium cation was used as a standard. The yield of the major isomer A was calculated based on the integration of three resonances: 4.5 ppm (t, 1H), 4.4 ppm (m, 1H), and 3.9 ppm (dd, 1H). The yield of the minor isomer B was calculated based on the integration of three resonances: 4.7 ppm (m, 1H), 4.0 ppm (t, 1H), and 3.5 ppm (dd, 1H). An impurity in the reaction mixture gives three resonances in the 2.5 – 5.0 ppm region, one of which overlaps with isomer A: 4.8 ppm (m, 1H), 4.5 ppm (t, 1H) and 3.9 ppm (dd, 1H).

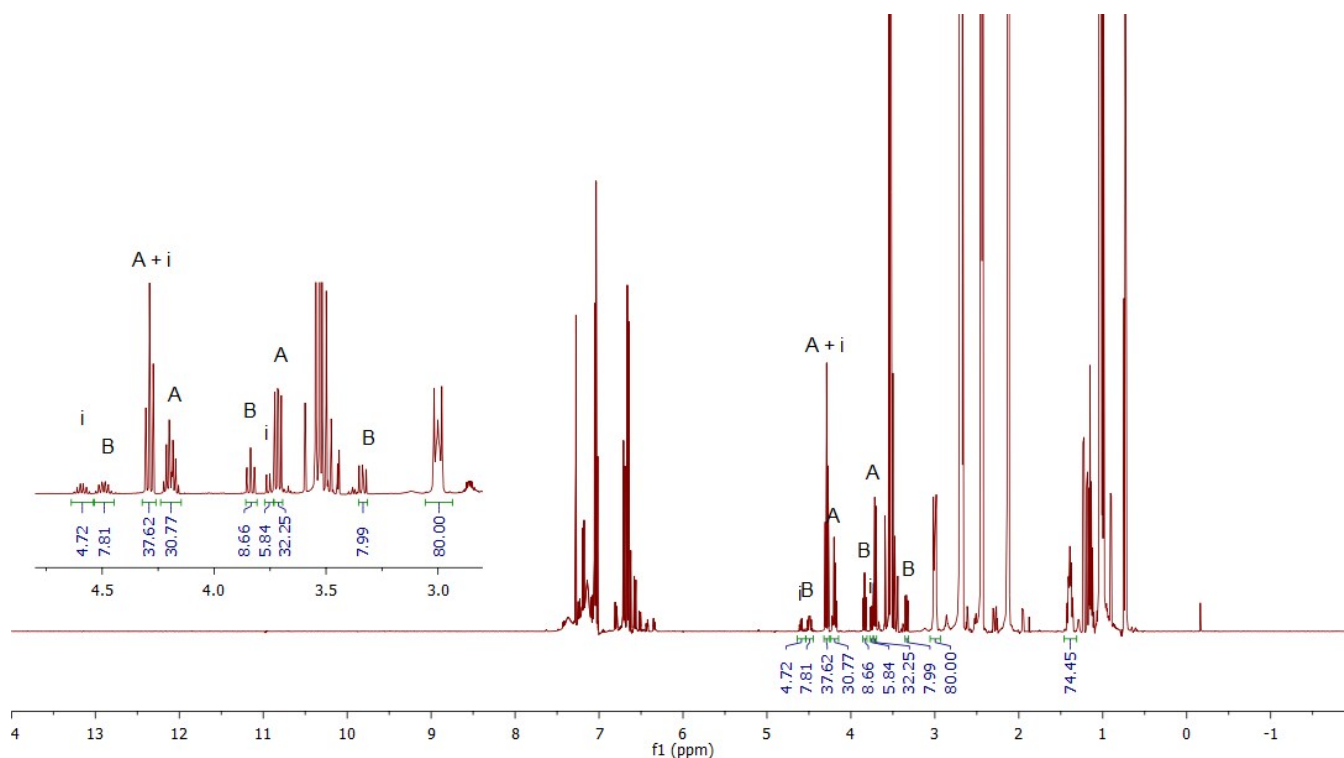


Figure S28. Representative ^1H NMR spectrum collected during the experiment presented in Table 2, Entry 3.

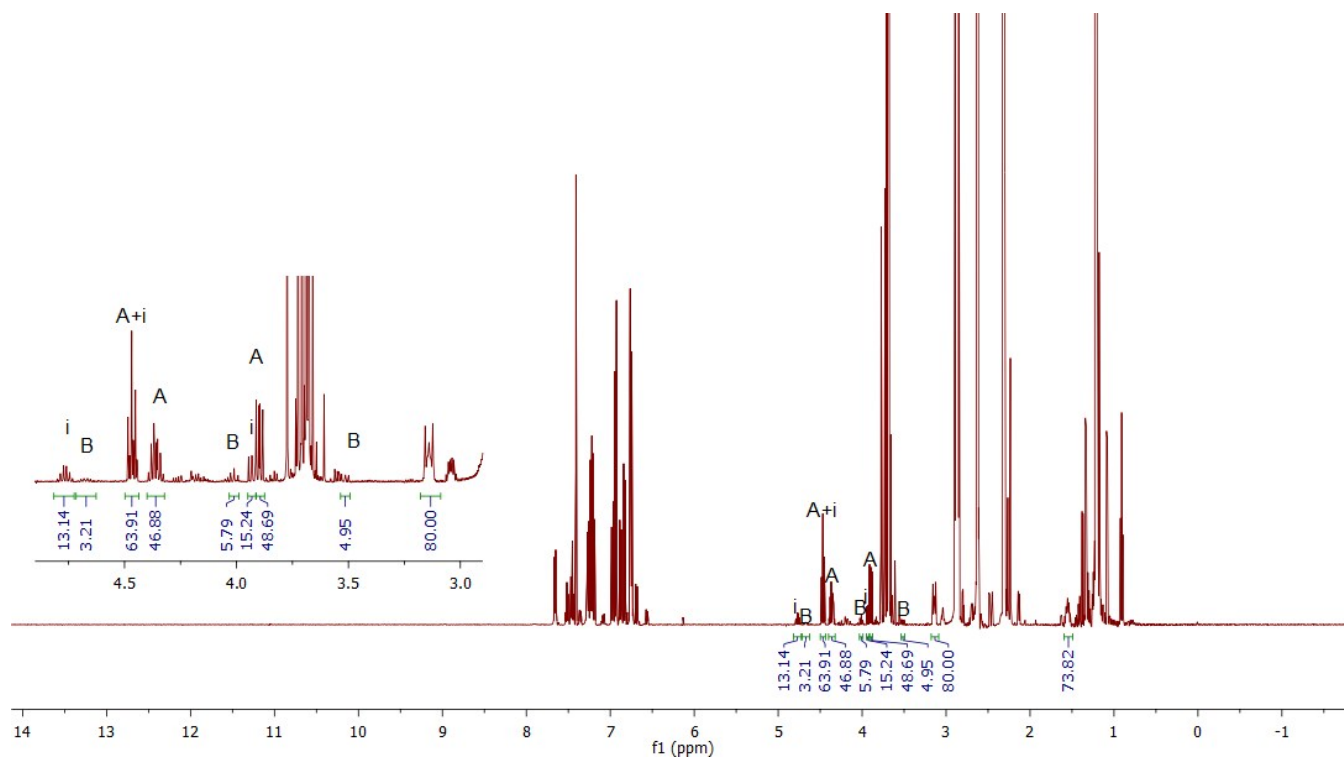
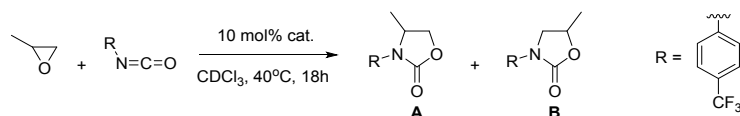


Figure S29. Representative ^1H NMR spectrum collected during the experiment presented in Table 2, Entry 4.

1.3.2.3 *In situ* NMR spectrum of Table 2, Entries 5-6



The formation of the products was monitored by ^1H NMR *in situ*. The integration of the resonance at 3.0 ppm (m, 12H) of the tetrabutylammonium cation was used as a standard. The yield of the major isomer A was calculated based on the integration of three resonances: 4.4 ppm (m, 1H), 4.3 ppm (t, 1H), and 3.8 ppm (dd, 1H). The yield of the minor isomer B was calculated based on the integration of three resonances: 4.6 ppm (m, 1H), 4.0 ppm (t, 1H), and 3.4 ppm (dd, 1H).

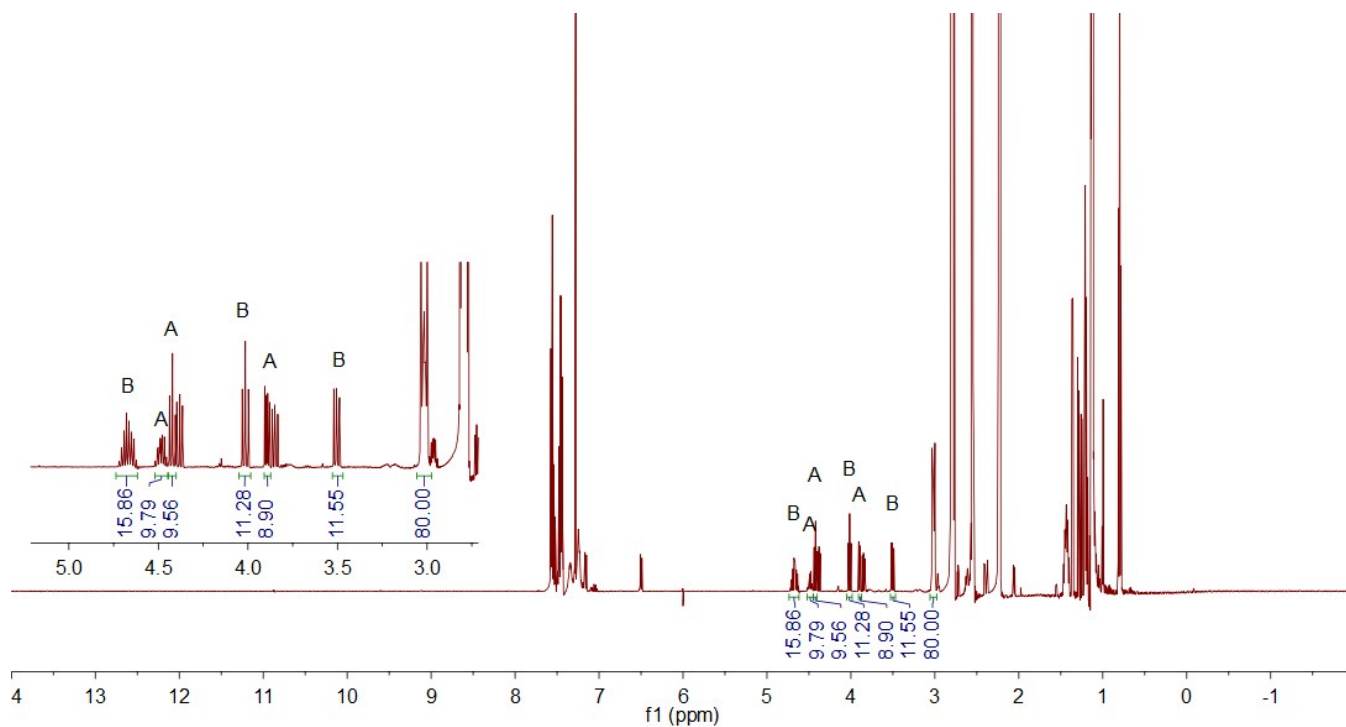


Figure S30. Representative ^1H NMR spectrum collected during the experiment presented in Table 2, Entry 5.

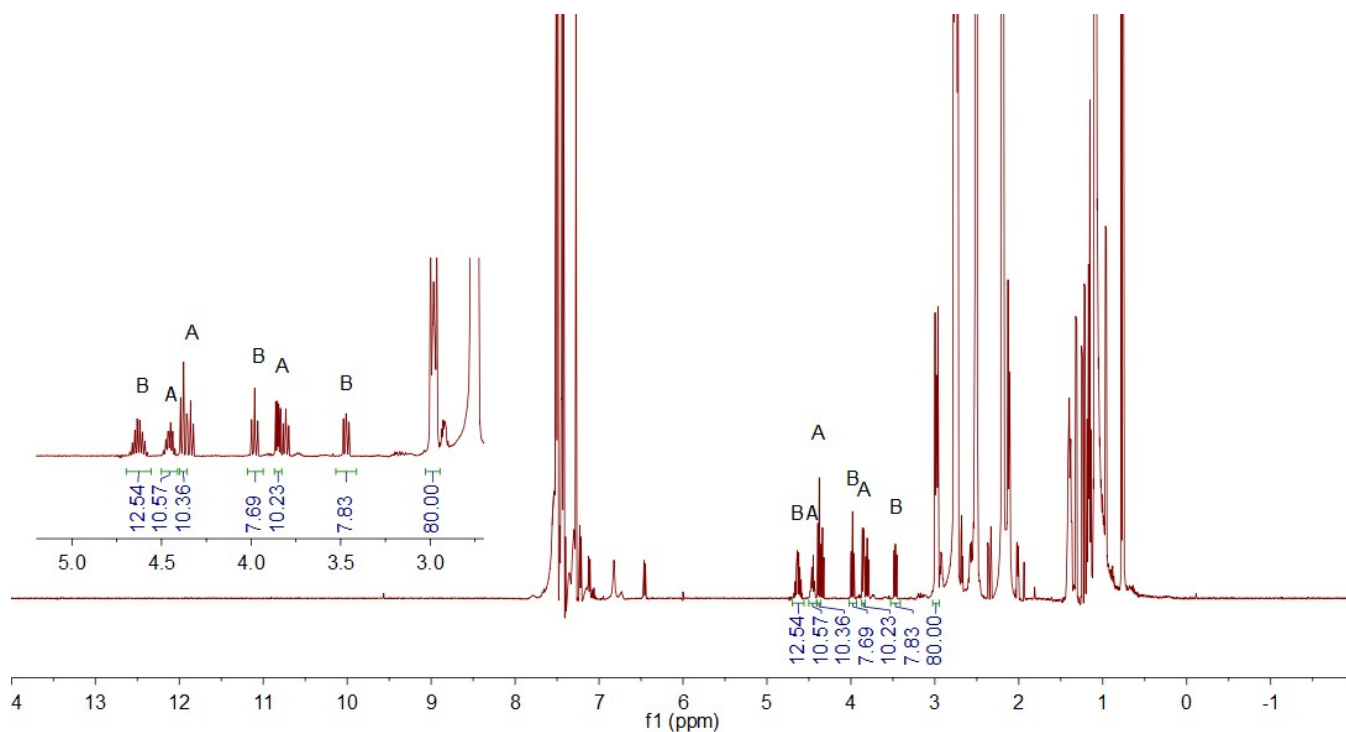
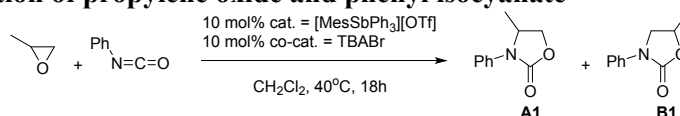


Figure S31. Representative ^1H NMR spectrum collected during the experiment presented in Table 2, Entry 6.

1.4 Catalytic cycloaddition of propylene oxide and phenyl isocyanate



To a stirred solution containing [MesSbPh₃][OTf] (150 mg, 0.24 mmol, 0.1 eq) and TBABr (77 mg, 0.24 mmol, 0.1 eq) in CH₂Cl₂ (5 mL), was added propylene oxide (2.5 mL, 36 mmol, 15 eq) and phenyl isocyanate (286 mg, 2.4 mmol, 1 eq). The reaction was stirred in a 40 °C bath for 18 h under N₂. An aliquot was taken from the reaction mixture and the yield of the two regioisomeric oxazolidinones was determined by ¹H NMR spectroscopy. The crude reaction mixture was subjected to flash chromatography over silica gel (3% ethyl acetate in hexanes). The third major fraction (very close to the second one) was collected washed with diethyl ether to afford product 5-methyl-3-phenyl-2-oxazolidinone (**B1**) as white powder (16 mg, 4%), and the fourth major fraction was collected to afford product 4-methyl-3-phenyl-2-oxazolidinone (**A1**) as colorless oil (170 mg, 40%).

4-methyl-3-phenyl-2-oxazolidinone (**A1**): ¹H NMR (500 MHz, CDCl₃) δ = 7.43 – 7.35 (m, 4H), 7.20 – 7.15 (m, 1H), 4.59 – 4.45 (m, 2H), 4.00 (dd, *J* = 7.8, 5.3, 1H), 1.30 (d, *J* = 5.9, 3H). ¹³C NMR (100 MHz, CDCl₃) δ = 155.82 (s), 136.60 (s), 129.27 (s), 125.32 (s), 122.04 (s), 68.76 (s), 52.42 (s), 18.54 (s). Spectral data are in accord with the previous report.²

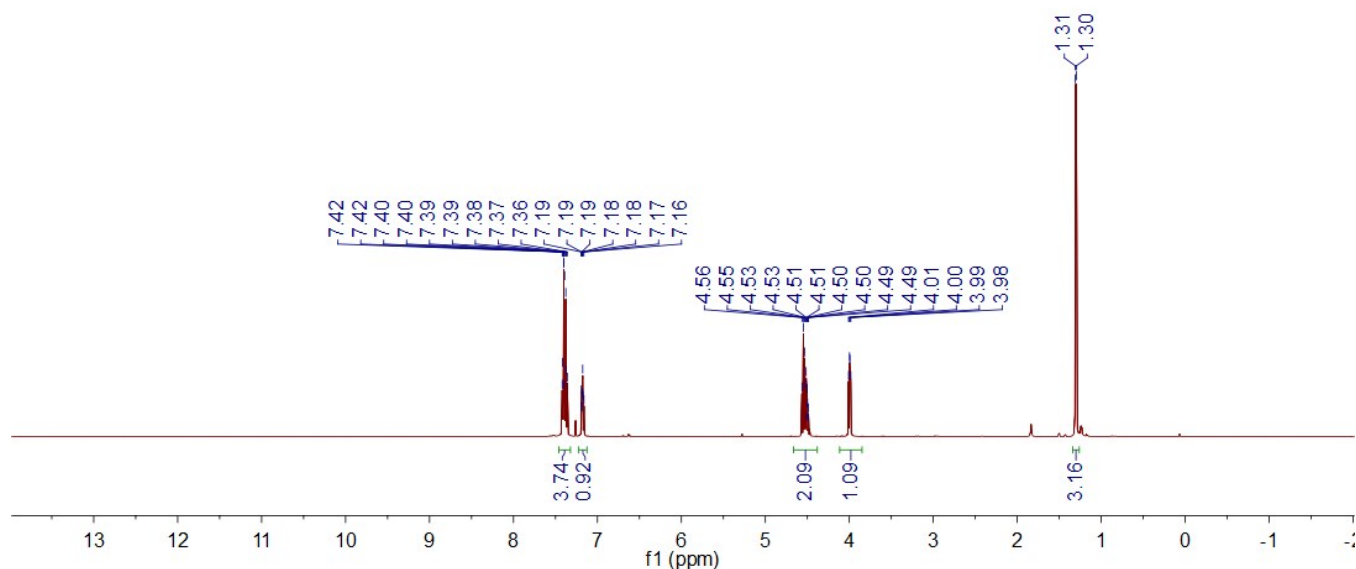


Figure S32. ¹H NMR of 4-methyl-3-phenyl-2-oxazolidinone (**A1**) in CDCl₃.

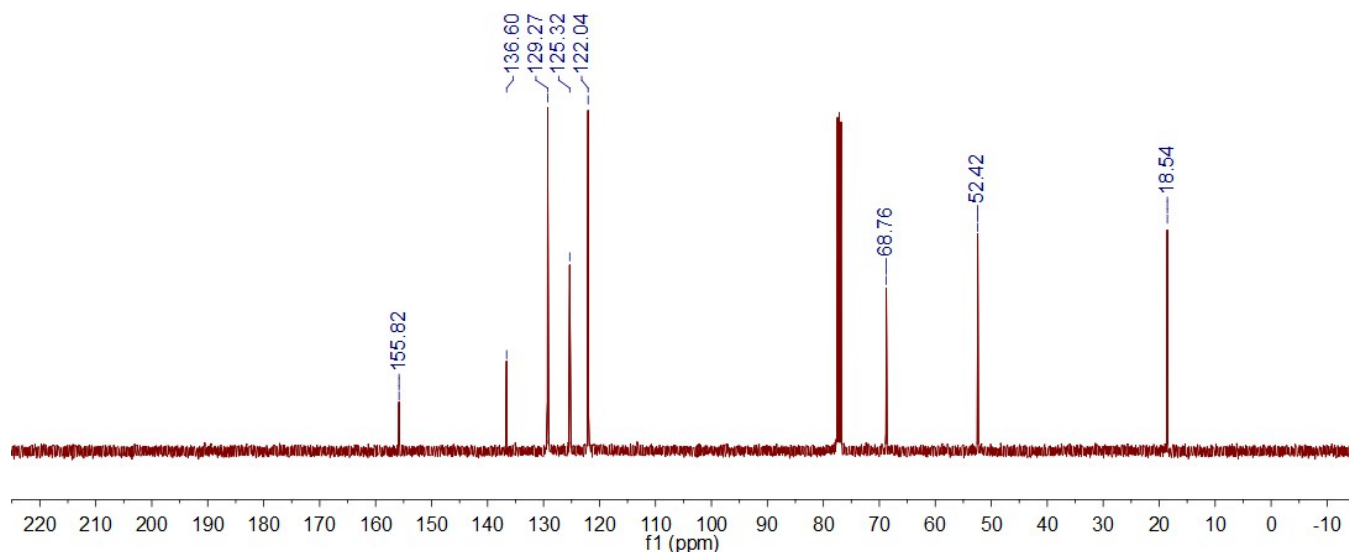


Figure S33. ^{13}C NMR of 4-methyl-3-phenyl-2-oxazolidinone (**A1**) in CDCl_3 .

5-methyl-3-phenyl-2-oxazolidinone (**B1**): ^1H NMR (500 MHz, CDCl_3) δ = 7.57 – 7.50 (m, 2H), 7.41 – 7.35 (m, 2H), 7.17 – 7.11 (m, 1H), 4.85 – 4.74 (m, 1H), 4.12 (t, J = 8.4, 1H), 3.63 (dd, J = 8.6, 7.1, 1H), 1.54 (d, J = 6.3, 1H). ^{13}C NMR (126 MHz, CDCl_3) δ = 155.01 (s), 138.51 (s), 129.18 (s), 124.09 (s), 118.31 (s), 69.66 (s), 52.03 (s), 20.87 (s). Spectral data are in accord with the previous report.²

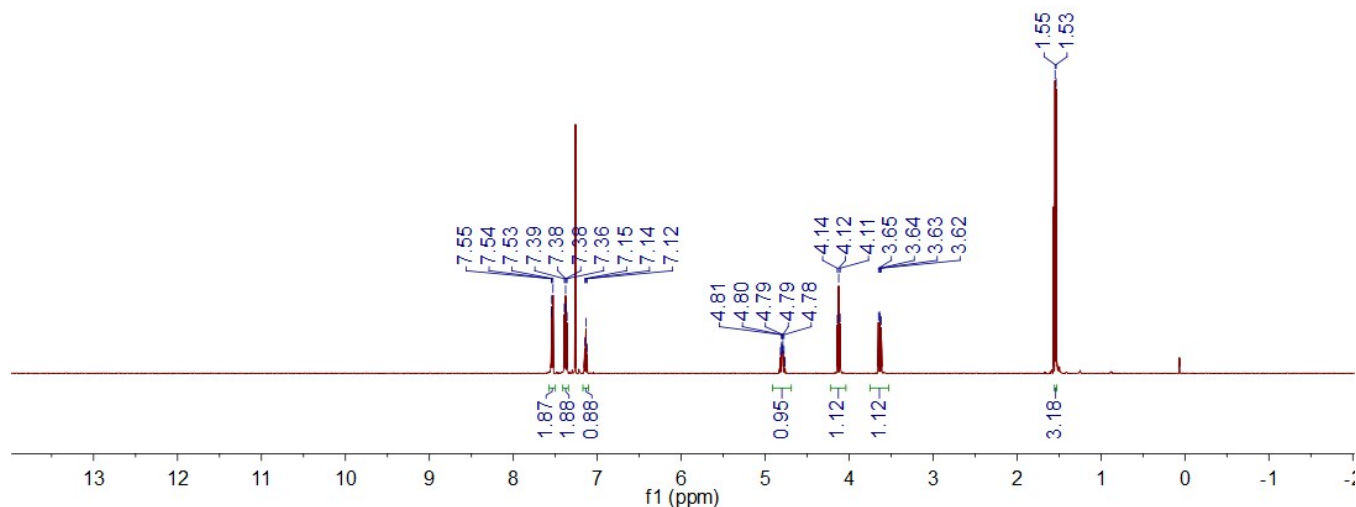


Figure S34. ^1H NMR of 5-methyl-3-phenyl-2-oxazolidinone (**B1**) in CDCl_3 .

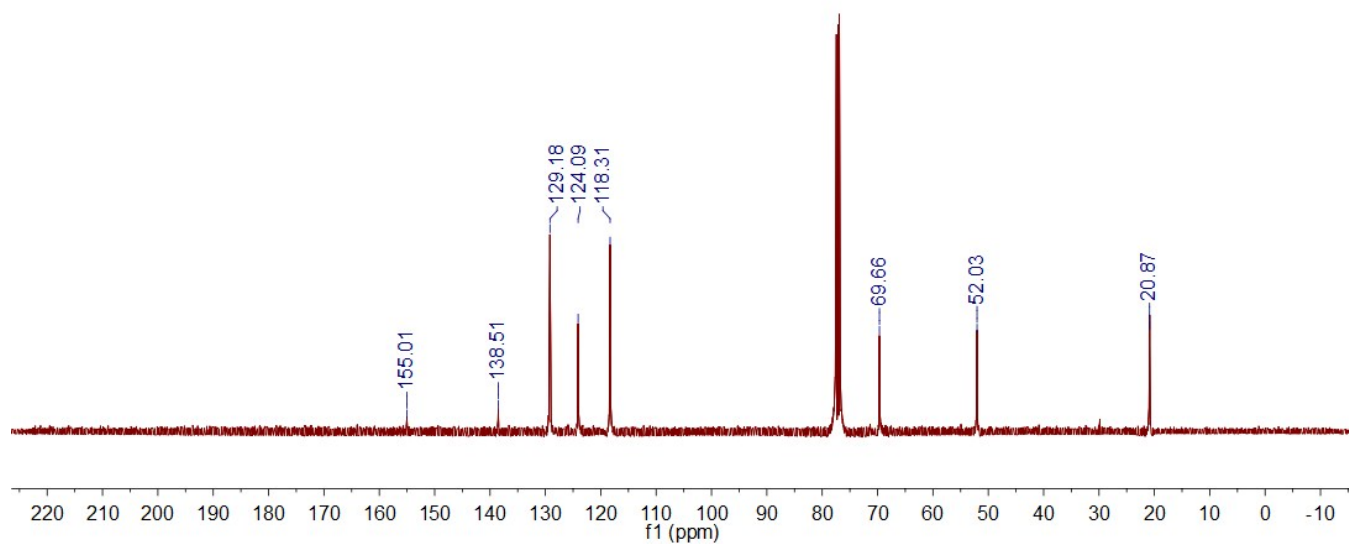
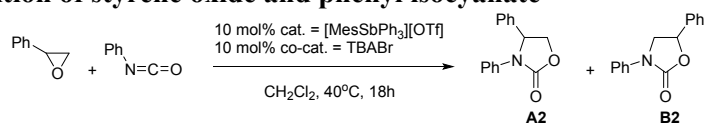


Figure S35. ¹³C NMR of 5-methyl-3-phenyl-2-oxazolidinone (**B1**) in CDCl₃.

1.5 Catalytic cycloaddition of styrene oxide and phenyl isocyanate



To a stirred solution of catalyst [MesSbPh₃][OTf] (125 mg, 0.20 mmol, 0.1 eq), co-catalyst TBABr (65 mg, 0.20 mmol, 0.1 eq) in CH₂Cl₂ (5 mL) was added styrene oxide (3.5 mL, 30 mmol, 15 eq) and phenyl isocyanate (243 mg, 2.0 mmol, 1 eq). The reaction was stirred in a 40 °C bath for 18 h under N₂. An aliquot was taken from the reaction mixture and the yield of two regioisomeric oxazolidinones was determined by ¹H NMR spectroscopy. The reaction mixture was treated to flash chromatography over silica gel (gradient 0-50% ethyl acetate in hexanes) and the third major fraction was collected and treated again to flash chromatography over silica gel (gradient 5-20% ethyl acetate in hexanes). The third major fraction was collected and recrystallized with diethyl ether to afford product 3,5-diphenyl-2-oxazolidinone (**B2**) as white powder (16 mg, 3%), and the fourth major fraction was collected and washed with hexanes to afford product 3,4-diphenyl-2-oxazolidinone (**A2**) as white powder (210 mg, 43%).

3,4-diphenyl-2-oxazolidinone (**A2**): ¹H NMR (500 MHz, CDCl₃) δ = 7.43 – 7.35 (m, 4H), 7.35 – 7.30 (m, 3H), 7.30 – 7.25 (m, 2H), 7.11 – 7.06 (m, 1H), 5.42 (dd, *J* = 8.7, 6.0, 1H), 4.80 (t, *J* = 8.7, 1H), 4.22 (dd, *J* = 8.7, 6.0, 1H). ¹³C NMR (126 MHz, CDCl₃) δ = 156.08 (s), 138.37 (s), 137.13 (s), 129.52 (s), 129.04 (s), 128.97 (s), 126.37 (s), 124.83 (s), 120.98 (s), 69.95 (s), 60.85 (s). Spectral data are in accord with the previous report.²

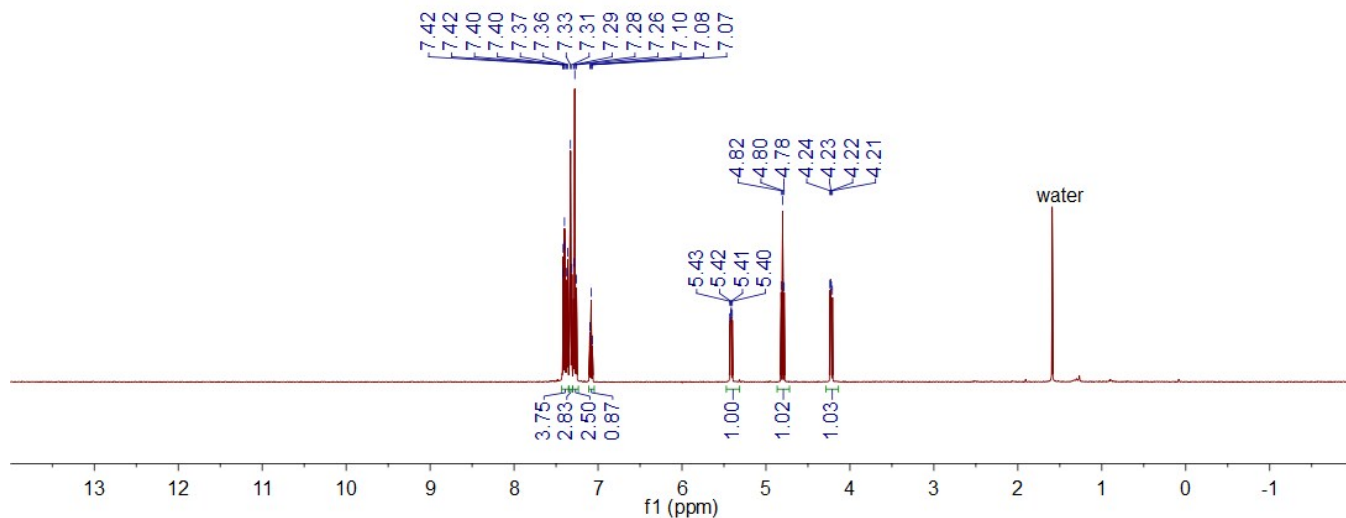


Figure S36. ¹H NMR of 3,4-diphenyl-2-oxazolidinone (**A2**) in CDCl₃.

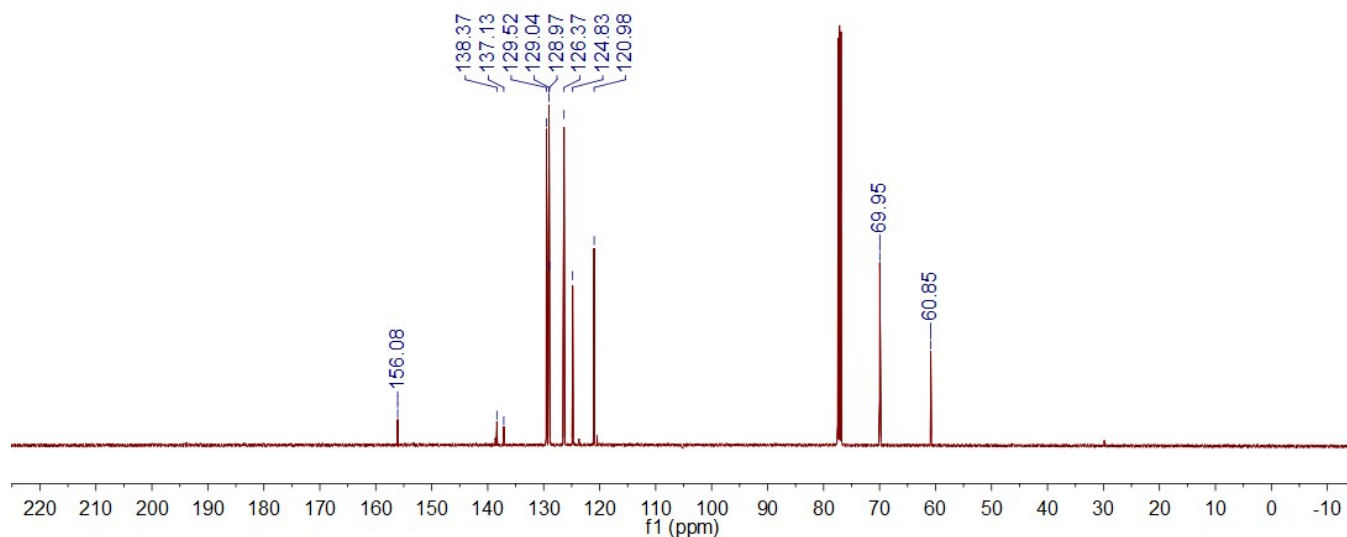


Figure S37. ^{13}C NMR of 3,4-diphenyl-2-oxazolidinone (**A2**) in CDCl_3 .

3,5-diphenyl-2-oxazolidinone (**B2**): ^1H NMR (500 MHz, CDCl_3) $\delta = 7.58 - 7.52$ (m, 2H), 7.48 – 7.36 (m, 7H), 7.19 – 7.12 (m, 1H), 5.65 (dd, $J = 8.8, 7.5$, 1H), 4.39 (t, $J = 8.8$, 1H), 3.98 (dd, $J = 8.8, 7.5$, 1H). ^{13}C NMR (126 MHz, CDCl_3) $\delta = 154.85$ (s), 138.27 (s), 138.24 (s), 129.28 (s), 129.27 (s), 129.20 (s), 125.83 (s), 124.35 (s), 118.45 (s), 74.19 (s), 52.88 (s). Spectral data are in accord with the previous report.²

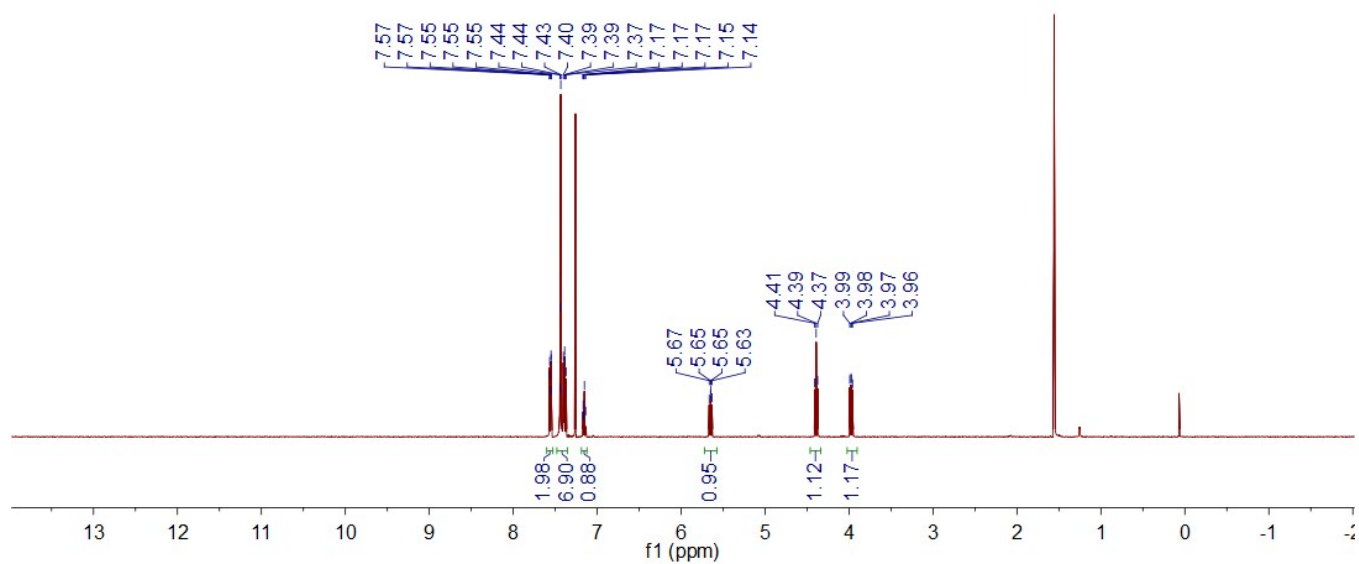


Figure S38. ^1H NMR of 3,5-diphenyl-2-oxazolidinone (**B2**) in CDCl_3 .

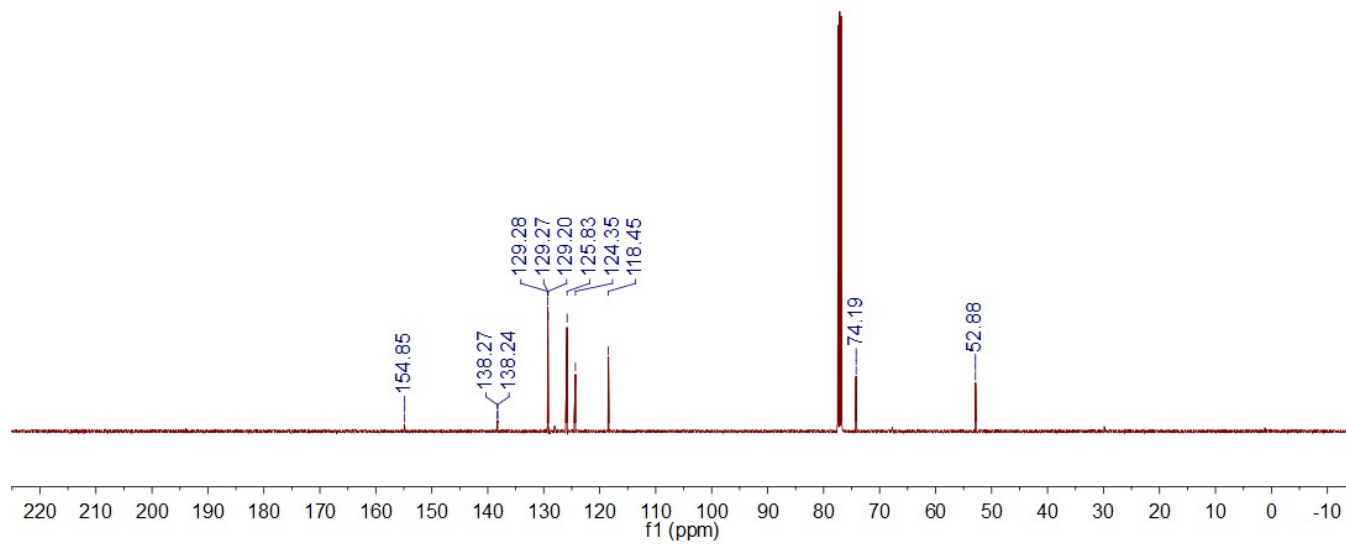


Figure S39. ^{13}C NMR of 3,5-diphenyl-2-oxazolidinone (**B2**) in CDCl_3 .

2 Crystallographic measurements.

2.1 1-Naphthyltriphenylstibonium triflate (2[OTf])

Table S1. Crystal data, data collection, and structure refinement for 2[OTf]

| | |
|-----------------------------------|--|
| Empirical formula | C ₂₉ H ₂₂ F ₃ O ₃ S Sb |
| Formula weight | 629.27 |
| Temperature | 110 K |
| Wavelength | 0.71073 Å |
| Crystal system | Monoclinic |
| Space group | C 1 2/c 1 |
| Unit cell dimensions | a = 14.848(7) Å b = 14.208(7) Å c = 24.673(17) Å α = 90°. β = 102.698(9)°. γ = 90°. |
| Volume | 5078(5) Å ³ |
| Z | 8 |
| Density (calculated) | 1.646 Mg/m ³ |
| Absorption coefficient | 1.221 mm ⁻¹ |
| F(000) | 2512 |
| Crystal size | 0.42 x 0.3 x 0.1 mm ³ |
| Theta range for data collection | 2.296 to 27.447°. |
| Index ranges | -18 < h < 18, -18 < k < 18, -31 < l < 31 |
| Reflections collected | 78867 |
| Independent reflections | 5413 [R(int) = 0.0800] |
| Completeness to theta = 25.242° | 99.9 % |
| Absorption correction | Semi-empirical from equivalents |
| Max. and min. transmission | 0.7455 and 0.5966 |
| Refinement method | Full-matrix least-squares on F ² |
| Data / restraints / parameters | 5413 / 121 / 437 |
| Goodness-of-fit on F ₂ | 1.025 |
| Final R indices [I > 2σ(I)] | R ₁ ^a = 0.0400, wR ₂ ^b = 0.0761 |
| R indices (all data) | R ₁ = 0.0769, wR ₂ = 0.0904 |
| Extinction coefficient | n/a |
| Largest diff. peak and hole | 0.575 and -0.538 e.Å ⁻³ |

^aR₁ = Σ||F_o| - |F_c|| / Σ|F_o|. ^bwR₂ = ([w(F_o² - F_c²)²] / [Σw(F_o²)²])^{1/2}; w = 1/[σ²(F_o²) + (ap)² + bp]; p = (F_o² + 2F_c²)/3 with a = 0.02430 and b = 20.4903.

2.2 [MesSbPh₃][OTf] (4[OTf])

Table S2. Crystal data, data collection, and structure refinement for 4[OTf]

| | |
|-----------------------------------|---|
| Empirical formula | C ₂₈ H ₂₆ F ₃ O ₃ S Sb |
| Formula weight | 621.30 |
| Temperature | 110 K |
| Wavelength | 0.71073 Å |
| Crystal system | Monoclinic |
| Space group | <i>P</i> 1 2 ₁ /n 1 |
| Unit cell dimensions | a = 11.4672(4) Å b = 19.4493(8) Å c = 11.7980(5) Å α = 90°. β = 95.029(2)°. γ = 90°. |
| Volume | 2621.17(18) Å ³ |
| Z | 4 |
| Density (calculated) | 1.574 Mg/m ³ |
| Absorption coefficient | 1.181 mm ⁻¹ |
| F(000) | 1248 |
| Crystal size | 0.36 x 0.29 x 0.1 mm ³ |
| Theta range for data collection | 2.025 to 27.900°. |
| Index ranges | -15 < h < 15, -25 < k < 25, -15 < l < 15 |
| Reflections collected | 96586 |
| Independent reflections | 6238 [R(int) = 0.0997] |
| Completeness to theta = 25.242° | 100.0 % |
| Absorption correction | Semi-empirical from equivalents |
| Max. and min. transmission | 0.7456 and 0.6324 |
| Refinement method | Full-matrix least-squares on F ² |
| Data / restraints / parameters | 6238 / 0 / 328 |
| Goodness-of-fit on F ² | 1.009 |
| Final R indices [I > 2σ(I)] | R ¹ = 0.0352, wR ² = 0.0756 |
| R indices (all data) | R ₁ = 0.0648, wR ₂ = 0.0885 |
| Extinction coefficient | n/a |
| Largest diff. peak and hole | 0.742 and -1.319 e.Å ⁻³ |

^a $R_1 = \sum ||F_o| - |F_c|| / \sum |F_o|$. ^b $wR_2 = ([\sum w(F_o^2 - F_c^2)^2] / [\sum w(F_o^2)^2])^{1/2}$; $w = 1/[\sigma^2(F_o^2) + (ap)^2 + bp]$; $p = (F_o^2 + 2F_c^2)/3$ with $a = 0.0370$ and $b = 4.2008$.

2.3 [(*o*-(Me₂N)C₆H₄)SbPh₃][OTf] (5 [OTf])

Table S3. Crystal data, data collection, and structure refinement for 5[OTf]

| | |
|-----------------------------------|--|
| Empirical formula | C ₂₇ H ₂₅ F ₃ N O ₃ S Sb |
| Formula weight | 622.29 |
| Temperature | 110.0 K |
| Wavelength | 0.71073 Å |
| Crystal system | Orthorhombic |
| Space group | Pbca |
| Unit cell dimensions | a = 18.642(2) Å b = 14.0067(18) Å c = 19.752(2) Å α = 90° β = 90° γ = 90° |
| Volume | 5157.5(10) Å ³ |
| Z | 8 |
| Density (calculated) | 1.603 Mg/m ³ |
| Absorption coefficient | 1.202 mm ⁻¹ |
| F(000) | 2496 |
| Crystal size | 0.45 x 0.05 x 0.04 mm ³ |
| Theta range for data collection | 2.062 to 27.974° |
| Index ranges | -24 < h < 24, -18 < k < 18, -25 < l < 25 |
| Reflections collected | 114700 |
| Independent reflections | 6139 [R(int) = 0.1617] |
| Completeness to theta = 25.242° | 100.0 % |
| Absorption correction | Semi-empirical from equivalents |
| Max. and min. transmission | 0.7456 and 0.5849 |
| Refinement method | Full-matrix least-squares on F ² |
| Data / restraints / parameters | 6139 / 0 / 328 |
| Goodness-of-fit on F ² | 1.049 |
| Final R indices [I > 2σ(I)] | R ¹ = 0.0448, wR ² = 0.1024 |
| R indices (all data) | R ₁ = 0.0722, wR ₂ = 0.1220 |
| Extinction coefficient | 0.00058(14) |
| Largest diff. peak and hole | 1.445 and -1.334 e.Å ⁻³ |

^a $R_1 = \sum ||F_o| - |F_c|| / \sum |F_o|$. ^b $wR_2 = ([\sum w(F_o^2 - F_c^2)^2] / [\sum w(F_o^2)^2])^{1/2}$; $w = 1/[\sigma^2(F_o^2) + (ap)^2 + bp]$; $p = (F_o^2 + 2F_c^2)/3$ with $a = 0.00313$ and $b = 14.5167$.

2.4 [(*o*-(Me₂NCH₂)C₆H₄)SbPh₃][OTf] (6[OTf])

Table S4. Crystal data, data collection, and structure refinement for 6[OTf]

| | |
|-----------------------------------|---|
| Empirical formula | C ₂₈ H ₂₇ F ₃ N O ₃ S Sb |
| Formula weight | 636.31 |
| Temperature | 110.0 K |
| Wavelength | 0.71073 Å |
| Crystal system | Monoclinic |
| Space group | <i>P</i> 1 2 ₁ /c 1 |
| Unit cell dimensions | a = 9.9453(7) Å b = 11.0052(8) Å c = 25.4792(17) Å α = 90° β = 101.217(4)° γ = 90° |
| Volume | 2735.4(3) Å ³ |
| Z | 4 |
| Density (calculated) | 1.545 Mg/m ³ |
| Absorption coefficient | 1.135 mm ⁻¹ |
| F(000) | 1280 |
| Crystal size | 0.55 x 0.1 x 0.1 mm ³ |
| Theta range for data collection | 1.630 to 27.696° |
| Index ranges | -12 < = h < = 12, -14 < = k < = 14, -33 < = l < = 33 |
| Reflections collected | 87657 |
| Independent reflections | 6349 [R(int) = 0.1112] |
| Completeness to theta = 25.242° | 100.0 % |
| Absorption correction | Semi-empirical from equivalents |
| Max. and min. transmission | 0.7455 and 0.5519 |
| Refinement method | Full-matrix least-squares on F ² |
| Data / restraints / parameters | 6349 / 205 / 392 |
| Goodness-of-fit on F ₂ | 1.171 |
| Final R indices [I > 2σ(I)] | R ₁ ^a = 0.0991, wR ₂ ^b = 0.1890 |
| R indices (all data) | R ₁ = 0.1296, wR ₂ = 0.2027 |
| Extinction coefficient | 0.0014(3) |
| Largest diff. peak and hole | 1.332 and -1.787 e.Å ⁻³ |

^a $R_1 = \sum ||F_o| - |F_c|| / \sum |F_o|$. ^b $wR_2 = ([\sum w(F_o^2 - F_c^2)^2] / [\sum w(F_o^2)^2])^{1/2}$; $w = 1 / [\sigma^2(F_o^2) + (ap)^2 + bp]$; $p = (F_o^2 + 2F_c^2) / 3$ with $a = 0.0001$ and $b = 35.9234$.

2.5 [Sb(C₆F₅)₄][SbCl₆] (7[SbCl₆])

Table S5. Crystal data, data collection, and structure refinement for 7[SbCl₆]

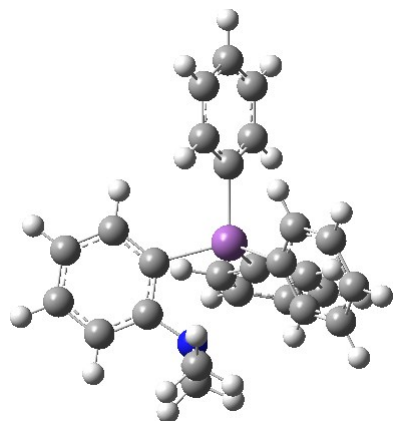
| | |
|-----------------------------------|--|
| Empirical formula | C ₂₄ Cl ₆ F ₂₀ Sb ₂ |
| Formula weight | 1124.44 |
| Temperature | 150(2) K |
| Wavelength | 0.71073 Å |
| Crystal system | Monoclinic |
| Space group | P 1 2 ₁ 1 |
| Unit cell dimensions | a = 17.482(4) Å b = 21.716(5) Å c = 19.115(4) Å α = 90° β = 116.456(6)° γ = 90° |
| Volume | 6497(3) Å ³ |
| Z | 8 |
| Density (calculated) | 2.299 Mg/m ³ |
| Absorption coefficient | 2.292 mm ⁻¹ |
| F(000) | 4224 |
| Crystal size | 0.426 x 0.186 x 0.092 mm ³ |
| Theta range for data collection | 1.19 to 30.66° |
| Index ranges | -25 < h < 24, -30 < k < 31, -27 < l < 27 |
| Reflections collected | 159165 |
| Independent reflections | 39702 [R(int) = 0.1041] |
| Completeness to theta = 30.66° | 99.1 % |
| Absorption correction | Semi-empirical from equivalents |
| Max. and min. transmission | 0.82 and 0.66 |
| Refinement method | Full-matrix least-squares on F ₂ |
| Data / restraints / parameters | 39702 / 1 / 1874 |
| Goodness-of-fit on F ₂ | 1.005 |
| Final R indices [I > 2σ(I)] | R ₁ ^a = 0.0472, wR ₂ ^b = 0.0922 |
| R indices (all data) | R ₁ = 0.0823, wR ₂ = 0.1167 |
| Absolute structure parameter | 0.143(16) |
| Largest diff. peak and hole | 1.079 and -1.346 e.Å ⁻³ |

^a $R_1 = \sum ||F_o| - |F_c|| / \sum |F_o|$. ^b $wR_2 = ([\sum w(F_o^2 - F_c^2)^2] / [\sum w(F_o^2)^2])^{1/2}$; $w = 1 / [\sigma^2(F_o^2) + (ap)^2 + bp]$; $p = (F_o^2 + 2F_c^2) / 3$ with $a = 0.0407$ and $b = 0.00$.

3 Computational Details

3.1 [(*o*-(Me₂N)C₆H₄)SbPh₃]⁺ (5⁺)

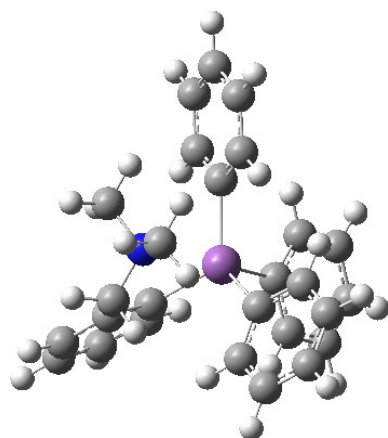
Table S6. XYZ coordinates of the optimized geometry of 5⁺



| | | | | | | | |
|----|-----------|-----------|-----------|---|-----------|-----------|-----------|
| Sb | 0.254890 | -0.029084 | -0.006581 | C | -0.483066 | 4.133824 | -1.060417 |
| N | -2.547314 | 0.205567 | -0.761231 | H | -1.241479 | 4.878500 | -0.832194 |
| C | 2.219894 | -0.780900 | -0.026817 | C | 0.610896 | 4.469802 | -1.861306 |
| C | 0.379618 | 1.889671 | -0.844290 | H | 0.700165 | 5.476862 | -2.260300 |
| C | -0.880363 | -1.524261 | -0.933158 | C | 1.593822 | 3.522298 | -2.143528 |
| C | -0.355350 | 0.137937 | 1.987810 | H | 2.449785 | 3.788554 | -2.757650 |
| C | 2.972294 | -0.826269 | 1.152339 | C | 1.487490 | 2.229875 | -1.627788 |
| H | 2.545561 | -0.490193 | 2.096662 | H | 2.273501 | 1.504385 | -1.830839 |
| C | 4.279939 | -1.312685 | 1.121446 | C | -0.959341 | -0.960008 | 2.612355 |
| H | 4.863959 | -1.349192 | 2.037216 | H | -1.134413 | -1.886417 | 2.065078 |
| C | 4.834473 | -1.750590 | -0.080989 | C | -1.348834 | -0.862689 | 3.947840 |
| H | 5.853303 | -2.128646 | -0.101513 | H | -1.818982 | -1.711677 | 4.437111 |
| C | 4.086165 | -1.707094 | -1.259013 | C | -1.135159 | 0.323286 | 4.652427 |
| H | 4.518493 | -2.051205 | -2.195025 | H | -1.441428 | 0.395698 | 5.692839 |
| C | 2.778997 | -1.223376 | -1.234223 | C | -0.530032 | 1.415131 | 4.029120 |
| H | 2.202089 | -1.200253 | -2.159649 | H | -0.362471 | 2.336525 | 4.580594 |
| C | -0.432736 | -2.810753 | -1.242615 | C | -0.136152 | 1.326155 | 2.693366 |
| H | 0.604368 | -3.097398 | -1.077313 | H | 0.335900 | 2.181797 | 2.211904 |
| C | -1.344568 | -3.731314 | -1.758952 | C | -2.905316 | 0.993952 | -1.949132 |
| H | -1.017089 | -4.737079 | -2.007404 | H | -2.078465 | 0.977696 | -2.667131 |
| C | -2.678106 | -3.362043 | -1.952562 | H | -3.087885 | 2.031558 | -1.651146 |
| H | -3.383193 | -4.084754 | -2.354946 | H | -3.812516 | 0.607205 | -2.439633 |
| C | -3.118399 | -2.076603 | -1.634983 | C | -3.604797 | 0.278086 | 0.255097 |
| H | -4.159781 | -1.801130 | -1.789629 | H | -4.578732 | -0.066211 | -0.127153 |
| C | -2.211609 | -1.149427 | -1.119073 | H | -3.710701 | 1.319416 | 0.579329 |
| C | -0.603618 | 2.841870 | -0.552243 | H | -3.327226 | -0.329859 | 1.121517 |
| H | -1.457812 | 2.576882 | 0.069296 | | | | |

3.2 $[(o\text{-}(\text{Me}_2\text{NCH}_2)\text{C}_6\text{H}_4)\text{SbPh}_3]^+$ (6^+)

Table S7. XYZ coordinates of the optimized geometry of 6^+



| | | | | | | | |
|----|-----------|-----------|-----------|---|-----------|-----------|-----------|
| Sb | 0.191784 | 0.031428 | 0.031696 | H | 2.812543 | 1.823920 | -0.286460 |
| C | -0.317577 | -0.808203 | 1.885290 | C | -0.481837 | -1.152035 | -1.576870 |
| C | -0.830813 | -2.109822 | 1.919697 | C | 0.453505 | -1.608879 | -2.512308 |
| H | -0.965639 | -2.679765 | 1.000225 | H | 1.506646 | -1.351349 | -2.412967 |
| N | -2.511747 | 0.321955 | -0.176014 | C | 0.038213 | -2.404677 | -3.580466 |
| C | -1.158943 | -2.693852 | 3.143546 | H | 0.764056 | -2.755299 | -4.309007 |
| H | -1.554611 | -3.705877 | 3.170654 | C | -1.307516 | -2.742479 | -3.706797 |
| C | -0.971701 | -1.981721 | 4.328650 | H | -1.637578 | -3.359500 | -4.538492 |
| H | -1.231182 | -2.436859 | 5.280941 | C | -2.238355 | -2.282264 | -2.774352 |
| C | -0.434041 | -0.694809 | 4.296391 | H | -3.290091 | -2.540585 | -2.884933 |
| H | -0.266937 | -0.149728 | 5.221731 | C | -1.839652 | -1.485225 | -1.701147 |
| C | -0.098919 | -0.107262 | 3.076325 | C | -2.852135 | -1.011580 | -0.681049 |
| H | 0.346188 | 0.886558 | 3.069391 | H | -3.864584 | -1.020675 | -1.119279 |
| C | 0.033282 | 2.117201 | -0.135574 | H | -2.872111 | -1.701395 | 0.173243 |
| C | -0.460847 | 2.904060 | 0.909299 | C | -3.253192 | 0.608786 | 1.057005 |
| H | -0.757744 | 2.457508 | 1.856487 | H | -3.001758 | 1.615841 | 1.405480 |
| C | -0.591398 | 4.282425 | 0.735067 | H | -2.983186 | -0.114243 | 1.834221 |
| H | -0.971601 | 4.895627 | 1.548090 | H | -4.341256 | 0.563594 | 0.887351 |
| C | -0.236658 | 4.870360 | -0.479682 | C | -2.828939 | 1.333490 | -1.195091 |
| H | -0.343998 | 5.943560 | -0.614143 | H | -2.589318 | 2.331040 | -0.815721 |
| C | 0.257833 | 4.084987 | -1.521564 | H | -3.898596 | 1.299161 | -1.457313 |
| H | 0.534705 | 4.542680 | -2.467793 | H | -2.240221 | 1.152108 | -2.101355 |
| C | 0.397897 | 2.707327 | -1.350686 | C | 4.558041 | 0.571103 | -0.191111 |
| H | 0.781913 | 2.102831 | -2.173289 | H | 5.246893 | 1.404604 | -0.301755 |
| C | 2.789026 | -1.567904 | 0.106972 | C | 5.046918 | -0.726347 | -0.049179 |
| H | 2.109286 | -2.412202 | 0.230353 | H | 6.119049 | -0.905435 | -0.051708 |
| C | 2.291179 | -0.265455 | -0.042406 | C | 4.163247 | -1.797342 | 0.101645 |
| C | 3.180904 | 0.804379 | -0.186049 | H | 4.545235 | -2.808216 | 0.218298 |

4 References

1. Arias Ugarte, R.; Devarajan, D.; Mushinski, R. M.; Hudnall, T. W., Antimony(v) cations for the selective catalytic transformation of aldehydes into symmetric ethers, α,β -unsaturated aldehydes, and 1,3,5-trioxanes. *Dalton Transactions* **2016**, 45 (27), 11150-11161.
2. Fujiwara, M.; Baba, A.; Matsuda, H., Selective α -cleavage cycloaddition of oxiranes with heterocumulenes catalyzed by tetraphenylstibonium iodide. *J. Heterocycl. Chem.* **1988**, 25 (5), 1351-1357.